Molecular Therapy
Nucleic Acids
Original Article

A pipeline for identifying guide RNA sequences that promote RNA editing of nonsense mutations that cause inherited retinal diseases

Nina Schneider,[1,3] Ricky Steinberg,[2,3] Amit Ben-David,[2,3] Johanna Valensi,[1,3] Galit David-Kadoch,[2] Zohar Rosenwasser,[2] Eyal Banin,[1] Erez Y. Levanon,[2] Dror Sharon,[1,3] and Shay Ben-Aroya[2,3]

[1]Division of Ophthalmology, Hadassah Medical Center, Faculty of Medicine, The Hebrew University of Jerusalem, Jerusalem 91120, Israel; [2]The Nano Center, The Mina and Everard Goodman Faculty of Life Sciences, Bar-Ilan University, Building 206, Room B-840, Ramat Gan 52900, Israel

Adenosine deaminases acting on RNA (ADARs) are endogenous enzymes catalyzing the deamination of adenosines to inosines, which are then read as guanosines during translation. This ability to recode makes ADAR an attractive therapeutic tool to edit genetic mutations and reprogram genetic information at the mRNA level. Using the endogenous ADARs and guiding them to a selected target has promising therapeutic potential. Indeed, different studies have reported several site-directed RNA-editing approaches for making targeted base changes in RNA molecules. The basic strategy has been to use guide RNAs (gRNAs) that hybridize and form a double-stranded RNA (dsRNA) structure with the desired RNA target because of ADAR activity in regions of dsRNA formation. Here we report on a novel pipeline for identifying disease-causing variants as candidates for RNA editing, using a yeast-based screening system to select efficient gRNAs for editing of nonsense mutations, and test them in a human cell line reporter system. We have used this pipeline to modify the sequence of transcripts carrying nonsense mutations that cause inherited retinal diseases in the *FAM161A*, *KIZ*, *TRPM1*, and *USH2A* genes. Our approach can serve as a basis for gene therapy intervention in knockin mouse models and ultimately in human patients.

INTRODUCTION

The most common type of RNA editing is the deamination of adenosine (A) to inosine (I), which is biochemically read as guanosine (G) by the translation machinery.[1] The consequence is an A-to-G substitution that can lead to codon changes (recoding)[2] and could rescue G-to-A mutations. A-to-I RNA editing is catalyzed by the highly conserved adenosine deaminase acting on RNA enzyme (ADAR) protein family, found in all metazoans.[3–6] In mammalians, the ADAR family consists of two active enzymes, ADAR1 and ADAR2, which share the catalytical deaminase domain (DD),[7] and double-stranded RNA (dsRNA) binding domains (RBDs). The RBDs bind not only to perfect dsRNA but also to imperfect double-stranded structures with mismatches at even higher affinity; accordingly, dsRNA is considered to be a prerequisite for editing by ADARs.[3,8]

In recent years, the prospect of using CRISPR-Cas9 for therapeutics has attracted much attention. This approach offers a solution to chronic conditions by introducing a lifelong permanent genetic modification.[9,10] However, in some cases, RNA editing could be a more appropriate alternative, as it does not require the introduction of foreign immunogenic prokaryotic proteins and any off-target effects are impermanent.[11] Thus, possible adverse effects would be reversible and tunable, making this approach safer.[12]

Advances made in understanding the mode of action of the ADAR proteins, enabled the development of several site-directed RNA-editing (SDRE) technologies as a therapeutic tool, one of which is by recruiting the endogenous ADAR, which is the method of choice in the present study. The ability of ADARs to recode makes them attractive therapeutic tools for correcting genetic mutations and reprogramming genetic information at the mRNA level. Several studies described pioneering approaches aiming to use ADAR-mediated editing as a therapeutic tool.[13,14] Given that most adenosines are not likely to occur in a proper structure for editing, the main challenge is to design guide RNAs (gRNAs), which form an artificial dsRNA structure around a user-defined target and redirect human ADAR (hADAR) activity to this site.

Inherited retinal diseases (IRDs) are a clinically heterogeneous and complex group of visual impairment phenotypes caused by pathogenic variants in at least 277 nuclear and mitochondrial genes causing vision loss in individuals worldwide.[15] It has been estimated that globally at least one in three individuals is a carrier of at least one recessive

Received 1 March 2023; accepted 24 January 2024;
https://doi.org/10.1016/j.omtn.2024.102130.

[3]These authors contributed equally

Correspondence: Dror Sharon, Division of Ophthalmology, Hadassah Medical Center, Faculty of Medicine, The Hebrew University of Jerusalem, Jerusalem 91120, Israel.
E-mail: dror.sharon1@mail.huji.ac.il
Correspondence: Shay Ben-Aroya, The Nano Center, The Mina and Everard Goodman Faculty of Life Sciences, Bar-Ilan University, Building 206, Room B-840, Ramat Gan 52900, Israel.
E-mail: Shay.Ben-Aroya@biu.ac.il

Table 1. Four ADARable nonsense IRD-causing mutations selected for the present study

Gene	NM	Inheritance pattern	gRNA	c.	p.	Number of patients in cohort	Original AA	Mutated AA[a]	ADAR edited AA[b]	% Editing ADAR1 (NGS)	% Editing ADAR2 (NGS)	% Editing ADAR1 (Sanger)	% Editing ADAR2 (Sanger)
TRPM1	NM_002420.5	AR	60 bases	c.880A>T	p.K294*	49	AAG (K)	**T**AG (*)	T**G**G (W)	32.6% (n = 8)	25.1% (n = 12)	42.4% (n = 10)	45.6% (n = 14)
FAM161A	NM_001201543	AR	60 bases	c.1567C>T	p.R523*	34	CGA (R)	**T**GA (*)	T**G**G (W)	2.5% (n = 2)	4.7% (n = 2)	1.7% (n = 2)	5.2% (n = 2)
KIZ	NM_018474.4	AR	60 bases	c.226C>T	p.R76*	21	CGA (R)	**T**GA (*)	T**G**G (W)	7.4% (n = 6)	7.8% (n = 6)	3.3% (n = 2)	9.9% (n = 3)
USH2A	NM_206933.2	AR	60 bases	c.11864G>A	p.W3955*	49[c]	TGG (W)	T**A**G (*)	T**G**G (W)	31.2% (n = 5)	20.5% (n = 4)	30.0% (n = 3)	29.5% (n = 5)
USH2A	NM_206933.2	AR	18 bases + 55 base GR	c.11864G>A	p.W3955*	49[c]	TGG (W)	T**A**G (*)	T**G**G (W)	0.5% (n = 2)	9% (n = 4)	0% (n = 2)	10.4% (n = 4)

AA, amino acid; AR, autosomal recessive; NGS, next-generation sequencing.
[a]The mutated nucleotide is in boldface type.
[b]The edited nucleotide is in boldface type.
[c]Based on a previous analysis of IRD variants worldwide.[15]

IRD-causing variant and that 1 in 1,380 individuals are affected by recessive IRDs.[16,17] Taking into account that ∼41% of IRD-causing single-nucleotide variants (SNVs) can be candidates for ADAR G-to-A editing,[15] the somewhat high editing activity in the retina,[18] and the relative ease of gRNA delivery to the retina, SDRE appears to be a promising approach for genetic therapy of IRDs. There is currently no effective treatment for the vast majority of IRDs, but recent adeno-associated virus (AAV)-based gene therapies bring some hope. Although this is the case, many relatively prevalent IRD-causing genes (such as *ABCA4* and *USH2A*) are too large for AAV vectors and/or have complex alternative splicing patterns yet to be well understood, and therefore new treatment modalities should be developed.

Here we developed a pipeline in which we selected common nonsense disease-causing mutations amenable for ADAR editing, used yeast screening systems that enable identification of efficient gRNAs that promote endogenous ADAR recruitment for SDRE, and verified their function in a human reporter cell line. Our study provides a proof of concept that RNA editing mediated by ADAR can be used as a novel approach for treating IRDs as well as other inherited diseases and forms the basis for better gRNA designs.

RESULTS

Selecting "ADARable" candidate mutations

We selected four nonsense mutations (Table 1) to be edited in the present study on the basis of the following rationale: optimal ADAR editing targets for this study were identified by using the previously reported coding system,[15] in which each SNV and therefore the corresponding mutated codon is assigned a score of 0–3, representing their amenability for undergoing ADAR editing. We assessed every disease-causing variant in a cohort of more than 2,100 Israeli and Palestinian families with IRDs as well as the international Global Retinal Inherited Disease (GRID) dataset.[15] Within our scoring system, a score of 3 denotes that the wild-type (WT) amino acid can be reinstated by ADAR editing, 2 denotes a nonsense mutation in a codon that can be edited to a missense variant by either correcting the mutated nucleotide or a neighboring nucleotide, 1 denotes a mutated codon causing a missense variant that can be edited to a different missense variant, and 0 denotes an amino acid that is unable to undergo editing to another amino acid. In our cohort, 47.4% of solved families with IRD-causing missense or nonsense mutations have a score of 3 or 2. The distribution of the ADAR score 2 variants in our cohort is shown in Figure 1. We chose the three most common Israeli editable nonsense mutations (in the *TRPM1*, *FAM161A*, and *KIZ* genes) within our cohort as targets (Table 1), all of which are score 2 mutations. In addition, we also chose the most common worldwide nonsense mutation (c.11864G>A; p.W3955* in *USH2A* with a score of 3), identified in at least 49 cases on the basis of our previous analysis.[15] All score 2 mutations had a neighboring adenosine whose subsequent deamination would transform the premature stop codon into a tryptophan (W), while the original *USH2A* codon can be reinstated by ADAR. Aiming to verify that the missense variants generated by RNA editing in the *KIZ*, *FAM161A*, and *TRPM1* genes are unlikely to affect protein function, we performed mutation and sequence analysis of these genes (Figure S1). Although these three particular amino acids are highly conserved, there are either no reported missense pathogenic variants (*KIZ*), a single "missense" mutation reported as pathogenic or likely pathogenic that is likely to affect splicing (*FAM161A*), or mainly null pathogenic variants (*TRPM1*) in these genes.

Creating a screening system in yeast for identifying the gRNA against IRD mutations

As a first step to identifying effective gRNAs for the aforementioned IRD-causing nonsense mutations, we created a yeast-based system to test candidate gRNAs (Figure 2A). The system is based on a strain carrying a *LEU2*-marked plasmid that can conditionally express hADAR1 or hADAR2 under a galactose-inducible promoter (*GAL1*p). This strain is a uracil auxotroph as a result of a deletion in the endogenous *URA3* gene, and thus is unable to grow in a medium lacking uracil. A second *HIS3*-marked plasmid carries a copy of a *URA3* gene that has

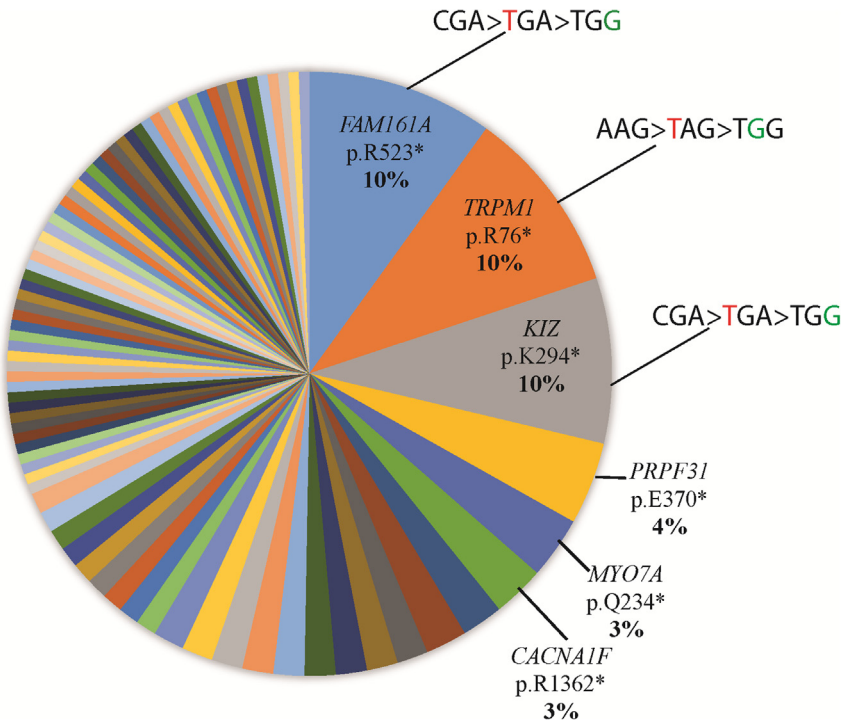

Figure 1. Most prevalent "ADARable" IRD-causing mutations with ADAR scores of 2 in our cohort calculated by percentage of families

The 3 most prevalent variants are also shown (original codon > mutated codon > edited codon).

been altered with a premature stop codon leading to the absence of the corresponding protein. This mutation was originated from 102 bp minigene fragments which were inserted in frame, immediately following the *URA3* start codon, and contain the nonsense mutation in the selected target genes (termed TRPM1-p.K294*-*ura3*, FAM161A-p.R523*-*ura3*, KIZ-p.R76*-*ura3*, and USH2A-p.W3955*-*ura3*). As shown in Figures 2C and 2D we validated that such insertions minimally affected the function of the *URA3* reporter gene. The 3′ end of the reporter gene is followed by a "tail" that can fold back and hybridize at the RNA level with the region flanking the nonsense mutation, thus creating a dsRNA structure that can promote ADAR-mediated editing of the UAG nonsense mutations, to UGG encoding tryptophan (Figure 2B). Thus, efficient hADAR-mediated editing of the IRD mutations should promote the expression of WT Ura3 and correlates with the strain's growth in uracil-depleted medium.

Both hADAR1 and hADAR2 exhibit high expression levels in the retina, surpassing those found in most other tissues, including various brain regions where editing activity is known to be relatively high (Figures S2A and S2B). ADAR2 is particularly abundant in the retina (Figure S2A), and as it is responsible for most of the recoding activity,[19–21] it is not surprising that the editing levels of the known recoding sites reach their peak in the retina (Figure S2C). Thus, we conducted experiments involving both hADAR1 and hADAR2.

To test whether the insertion of the minigene fragment affects the functionality of the *URA3* reporter gene, a positive control strain was created as well, in which the stop codon within the 102 bp fragment was swapped with tryptophan (TGG), mimicking the outcome of perfect editing of the target adenosine (TRPM1-K294W-*URA3*, FAM161A-R523W-*URA3*, KIZ-R76W-*URA3*, and USH2A-W3955W-*URA3*) (Figures 2C and 2D). This would lead to a full-length Ura3 protein carrying an extra 34 amino acids. As shown in Figures 2C and 2D, we were able to validate that this addition had only a minor effect on the growth rates in the absence of uracil and revealed the expected maximum growth associated with each insertion.

Next, we identified and optimized the gRNA sequence for each IRD mutation. As mentioned above, the gRNAs used in previous studies to direct the endogenous ADARs are composed of two essential elements: the "specificity domain" and a 49 nt dsRNA structure originating from the GluR (GR) ion channel receptors used to recruit ADAR binding (the "recruitment element"). We decided to test the following gRNAs (Figure 3A) for each of the IRD mutations: (1) a 60 nt sequence representing the specificity domain, which fully complements the cDNA of the IRD sequence (termed 60nt-SpD), except for an A-C mismatch at the target adenosine, which is known to enhance editing efficiency,[22] and (2) a shorter 30 nt specificity domain combined with GR as the recruiting element (termed 30nt-SpD-GR). These gRNAs were inserted in the above-mentioned 3′ end region. Next, we tested the growth of the indicated strains in the presence of galactose to induce hADAR2 or hADAR1 expression and under uracil depletion, for 25 hours. Growth was compared with the positive control carrying the corrected version of the IRD mutation (see above) and to the negative control carrying an empty *LEU2*-marked plasmid (without the hADAR) (Figure 3B). The results indicate that in the cases of *TRPM1*-p.K294* and *USH2A*-p.W3955*, the 60nt-SpD induced growth similar to the WT, while the 30nt-SpD-GR gRNA induced mild growth only in the case of the *USH2A* variant. However, the 60nt-SpD gRNA induced only minimal or mild growth in the cases of *KIZ*-p.R76* and *FAM161A* p.R523*, respectively (Figures 3C and 3D). No improvement was detected in the growth of these mutants even when we attempted to elongate the specificity domain to 60 nt and add GR as the recruiting element (60nt-SpD-GR) (Figure S3).

To validate the necessity of dsRNA formation in the vicinity of the target adenosine as an editing substrate for ADAR, we used a similar 60nt-SpD gRNA that in addition to the A-C mismatch, carried additional mismatches around the target adenosine. In comparison with the 60nt-SpD gRNA strain, which did not contain additional mismatches

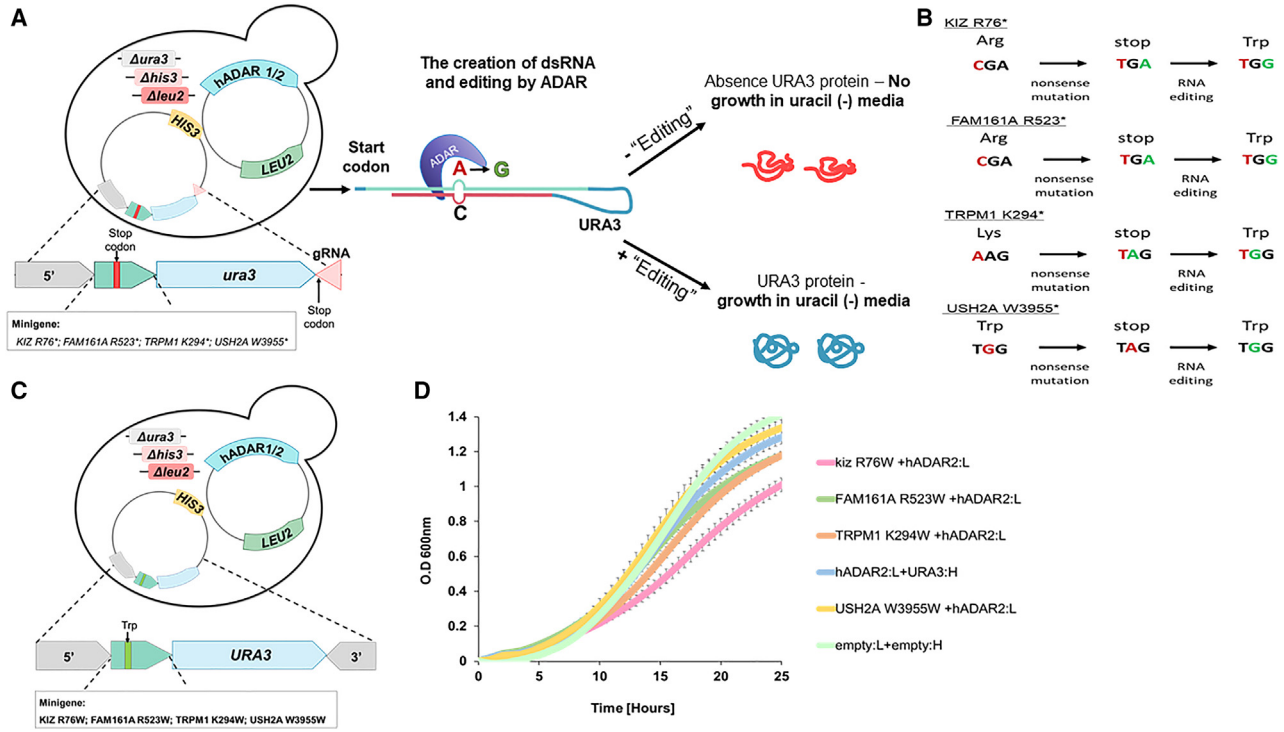

Figure 2. Yeast-based screening system for testing gRNAs that promote A-to-I editing

(A) Schematic representation of the yeast-based selection system. A uracil auxotroph yeast strain (deleted in the *URA3* genes [Δ*ura3*]) harbors a *LEU2*-marked plasmid that enables the conditional expression of hADAR2 or hADAR2 under a galactose-inducible promoter (*GAL1*p-hADAR1/2) and a *HIS3*-marked plasmid carrying the gene *URA3* as a reporter gene. The reporter gene expression was interrupted by the in-frame insertion of 102 bp minigene fragments containing the following nonsense mutations: TRPM1 K294*, FAM161A R523*, KIZ R76*, and USH2A W3955* (denoted by the green arrow with the red bar). The 3′ end of each plasmid containing the mutated insert is followed by a reverse complement gRNA sequence ("tail") of the region flanking the mutated insert (denoted a pink triangle in the *HIS3*-marked plasmid). When the "tail" folds back at the RNA level, it hybridizes with the corresponding mutated insert sequence and forms the dsRNA structure required for hADAR recruitment and editing, except from a single A-C mismatch at the target adenosine. If RNA editing is efficient, the translated wild-type Ura3 protein permits growth in a medium lacking uracil. (B) Sequences of the original amino acids, the specific changes leading to a nonsense mutation within the indicated mutations, and the result of ADAR-mediated editing. Nucleotides colored in red denote the specific mutation site. The target adenosines and the result of the ADAR-mediated editing are denoted in green. (C and D) Insertion of the corrected version of the minigene fragments minimally affect the function of the *URA3* reporter gene. (C) Similar to (A), the corrected version of the mutated insert (*>Trp) is denoted by the green bar. (D) Growth curves of the strains indicated in (C). Strains were grown to stationary phase in selective media supplemented with 2% raffinose (ADAR expression is off) and transferred to selective media lacking uracil, supplemented with 2% galactose (t-0) to induce the expression of hADAR2. Samples were brought to an optical density at a wavelength of 600 nm (O.D 600 nm) of 0.1, and the growth rate was assessed in a 96-well plate using a Tecan microplate reader by measuring O.D 600 nm every 30 min for 25 hours. Error bars represent the SD between three independent experiments. A plasmid carrying the *URA3* gene without the in-frame insertion of the mutated insert fragment was used as a positive control.

(termed "perfect tail"), we observed that the growth was largely impaired (Figure S4).

Overall, these results demonstrate that the combination of either hADAR2 or hADAR1, along with the hybridization of the dsRNA, can induce editing within the selected targets.

Next-generation sequencing confirms that yeast growth is associated with A-to-I editing

Next, we used next-generation sequencing (NGS) to validate that the yeast growth seen in our experimental system is a result of A-to-I editing carried out by hADAR2. To this end, we extracted RNA from the strains in which the presence of the selected IRD mutation, hADAR2, and either the gRNA 60nt-SpD (for variants in *FAM161A*, *TRPM1*, *KIZ*, and *USH2A*) or 30nt-SpD-GR (*USH2A*) induced yeast growth. cDNA of the region flanking the mutation was then amplified and subjected to NGS. The results indicate that in all cases, A-to-I editing at the target adenosine was detected. Strains carrying the *FAM161A* and *KIZ* variants exhibited the lowest editing levels of 5% and 1% (ADAR2), or 5% and 2.5% (ADAR1), which aligned with their limited growth, most probably because these mutants carry guanosines at the 5′ end of the target adenosine, which are largely depleted from the 5′ end of natively edited adenosines.[23] The *TRPM1* and *USH2A* variants showed a similar growth rate, with higher editing levels of 11% and 10% (ADAR2), or 40% and 30% (ADAR1), respectively, in the presence of the 60nt-SpD gRNA. Additionally, the presence of 30nt-SpD-GR induced editing levels of 0% and 7.3% (ADAR2), or 10.3% and 16% (ADAR1) (Figures 3C and 3D).

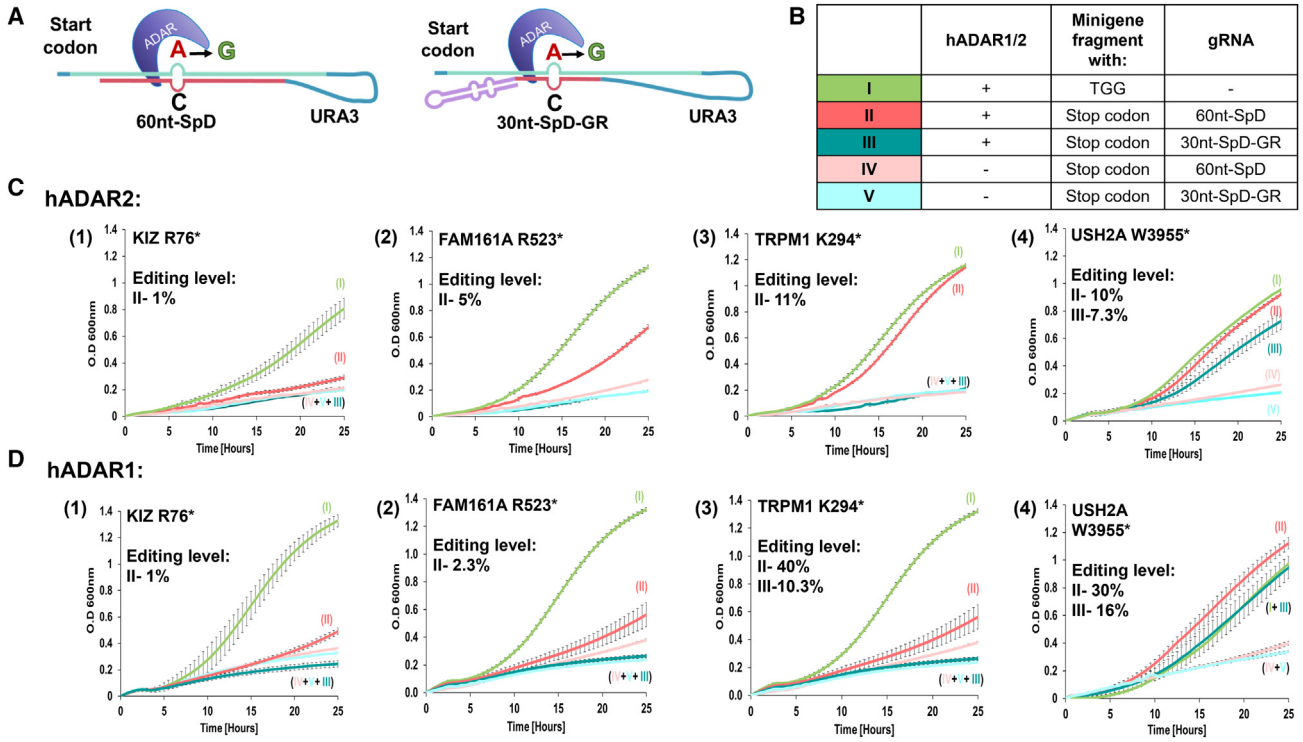

	hADAR1/2	Minigene fragment with:	gRNA
I	+	TGG	-
II	+	Stop codon	60nt-SpD
III	+	Stop codon	30nt-SpD-GR
IV	-	Stop codon	60nt-SpD
V	-	Stop codon	30nt-SpD-GR

Figure 3. hADAR2- and hADAR1-mediated editing of selected IRD mutations can be induced in the presence of gRNAs

(A) Schematic representation of the dsRNA structure formed when the "tail" containing the selected gRNA sequences folds back at the RNA level on the target to form the dsRNA structure for ADAR recruitment. (B) A table describing the contents of the strains (denoted as I–V) tested in (C)–(F). Strain I mimicked the outcome of perfect editing by ADAR and served as the positive control, while the negative controls (strains IV and V) carried an "hADAR1-mediated editing of selected empty" *LEU2* plasmid without the ADAR enzyme. (C and D) Growth curves of the indicated strains were produced as described in two dimensions in the presence of hADAR2 (top) and hADAR1 (bottom). The numbers representing the editing levels at the target A's are the average (n = 3) obtained on NGS analysis.

Overall, these results imply that the growth rate of the yeast strains in our screening system correlates with editing levels.

Expanding the yeast-based system for screening millions of candidate gRNAs

In naturally occurring editing sites, the dsRNA structure is imperfect in the vicinity of the targeted adenosine, and these mismatches are essential for efficient editing.[24,25] Thus, although it is clear that perfect RNA duplexes make suboptimal structures for editing, the positions of the mismatches and bulges are difficult to predict. Hence, we aimed to investigate whether our yeast strains could be employed for their identification.

As a control, we initiated by introducing a specific G-G mismatch between the target and gRNA at the 5′ G of the adenosine to be edited in *KIZ*-p.R76* and *FAM161A* p.R523* mutants. It was recently demonstrated that such a mismatch can enhance editing efficiency in this context.[26] Indeed, the results indicate a significant improvement in growth, which was correlated with increased editing efficiency 1%–38% (hADAR1) or 35% (hADAR2) in *KIZ*-p.R76* and 2.5%–10% (hADAR1), or 5%–8.6% (hADAR2), in *FAM161A* p.R523* (Figure 4). These findings underscore the potential of identifying specific mismatches that can enhance editing.

Next, we conducted an unbiased screening assay to identify the best performing gRNAs out of randomized pools. For this purpose, we focused on the *KIZ*-p.R76* mutant, which exhibited the lowest editing levels. We tested whether we could enhance the baseline editing levels obtained with the 60nt-SpD in the presence of hADAR2. To achieve this, we used the yeast strain described in Figure 2 to create a library of approximately 10^7 strains (Figure 5A). Each of these strains carries a distinct gRNA sequence that is mostly base-paired with the target, containing $\leq$6% mismatched positions, in addition to the A-C mismatch in the target adenosine. The 5′ and 3′ positions were left untouched, as we wanted to identify additional mismatches that could further contribute to the effect provided by the G:G mismatch at the 5′ G of the target as described above (see Figure 4). The library was then pooled and subjected to successive rounds of selection under uracil starvation (Figure 5B). Next, in order to identify the gRNA sequences responsible for enhancing editing and stimulating induced growth of cells in the pooled culture, we serially diluted a sample from the library and plated single cells on a medium that selects for the plasmid harboring the gRNAs and hADAR2. The sequences of

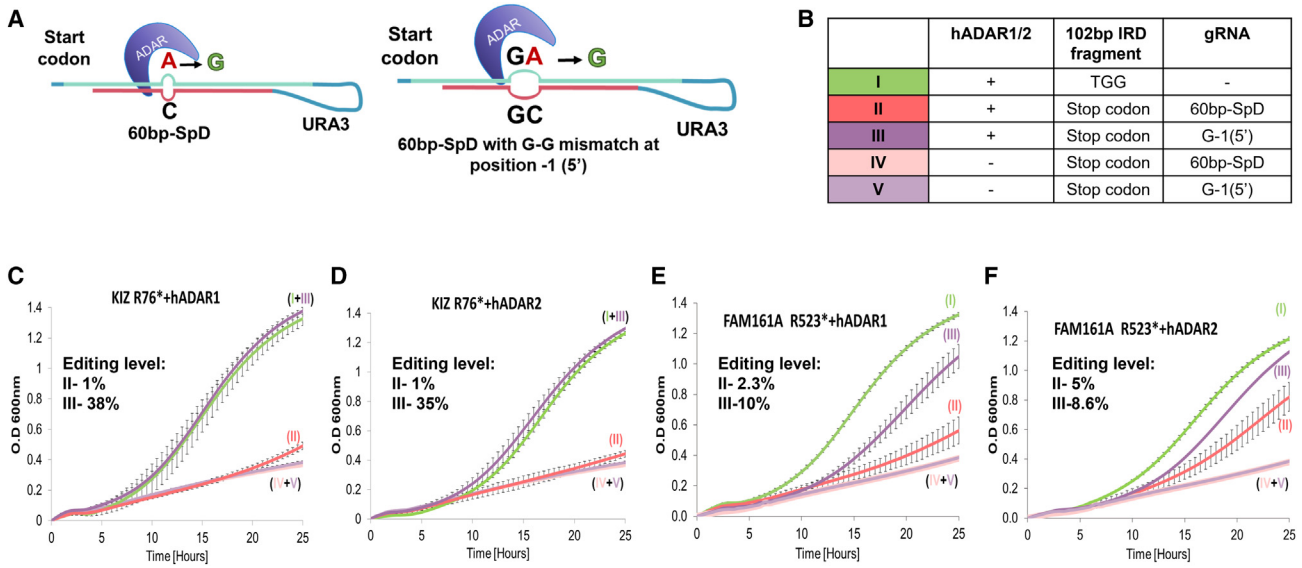

	hADAR1/2	102bp IRD fragment	gRNA
I	+	TGG	-
II	+	Stop codon	60bp-SpD
III	+	Stop codon	G-1(5')
IV	-	Stop codon	60bp-SpD
V	-	Stop codon	G-1(5')

Figure 4. Induction of editing with a G-G mismatch at the 5′ end of the target adenosine

Similar to Figure 3, but this time, the 60nt-SpD gRNA was compared with a gRNA containing a specific G-G mismatch between the target and gRNA at the 5′ G of the adenosine to be edited in KIZ-p.R76* and FAM161A p.R523* mutants (60nt-SpD G-G).

the gRNAs that facilitated growth in the selected colonies were determined through Sanger sequencing of the PCR products, using universal primers flanking the insertion sites of the gRNA-encoding DNA. NGS analysis of RNA samples extracted from the cells containing the identified mismatched gRNAs (dubbed "B4," "B12," and "TT") revealed that the minimal baseline editing level of 1% induced by the hADAR2 and 60nt-SpD was significantly increased to 4.5%–6% (Figure 5C).

These results along with the validation in mammalian cells (see below), demonstrate that our screening system can be scaled up and customized for screening millions of candidate gRNAs to identify those that are particularly efficient in editing selected targets.

Confirming a functional reporter system

As the gRNAs identified as ADAR-recruiting candidates for the specific genes and mutations were tested in a yeast system, we chose to then test these in a mammalian cell line using a fluorescent reporter system. Validation of the fluorescent reporter system was done by cloning a 161 nt gene fragment of the *GAPDH* 3′ UTR into the pmCherry-EGFP reporter plasmid. Although this part of the gene is not translated, we cloned it into a reading frame in which one of the only two "stop codons" contains the target adenosine (supplemental methods), whose place in the sequence would cause termination of translation unless edited. We made a single base change (T>C) to the other "stop codon" in the 3′ UTR, 8 nt downstream to the target adenosine, to prevent termination of translation (TAG>CAG) unrelated to RNA editing. A chemically modified gRNA with an 18 nt long complementarity region and a 55 nt GR motif tail targeting the specific adenosine in the reporter plasmid, previously developed by the Stafforst group,[27] was introduced to ADAR1 p.110 and ADAR2 (supplemental methods) overexpressing HeLa cells transiently transfected with the target plasmid, and all experimental wells showed both mCherry and EGFP fluorescence (Figure S5), while the negative control only showed mCherry fluorescence. Sanger sequencing showed that ADAR1 p.110-overexpressing and ADAR2-overexpressing HeLa cells underwent an average of 16.5% (n = 2) and 26.1% (n = 2) editing, respectively.

Editing levels are sequence dependent

Using our validated cellular reporter system in which a target nonsense mutation and surrounding exonic bases were inserted as a cassette between mCherry and EGFP in an expression plasmid and transfected into ADAR1 p.110-overexpressing and ADAR2-overexpressing HeLa cells, allowed us to measure the editing of our designed gRNAs (Figure 6A). The gRNAs used were those with the highest levels of editing and survival measured in the aforementioned yeast model. Introducing chemically modified 60-base oligomer gRNAs without a GR motif into ADAR1 p.110 or ADAR2-overexpressing stable HeLa cell lines induced varying levels of RNA editing.

The highest levels of editing were observed in the samples transfected with a *TRPM1* 60-mer gRNA as measured by both Sanger sequencing and NGS. The minigene reporter construct expressed in the cell lines contained the *TRPM1* mutation (c.880A>T, p.K294*) and the target adenosine for editing was the 3′ neighboring base to the mutated A>T (Table 1). Both mCherry and EGFP expression were observed in all samples (Figure 6B). For samples of gRNA-treated ADAR1 p.110-overexpressing HeLa cells in which RNA editing was clearly observed, an average of 42.4% (n = 10) and 32.6% (n = 8) editing was observed in Sanger sequencing and NGS, respectively, compared with an average of 45.6% (n = 14) and 25.1% (n = 12) editing observed among HeLa cells expressing ADAR2 in Sanger sequencing and NGS with the maximum

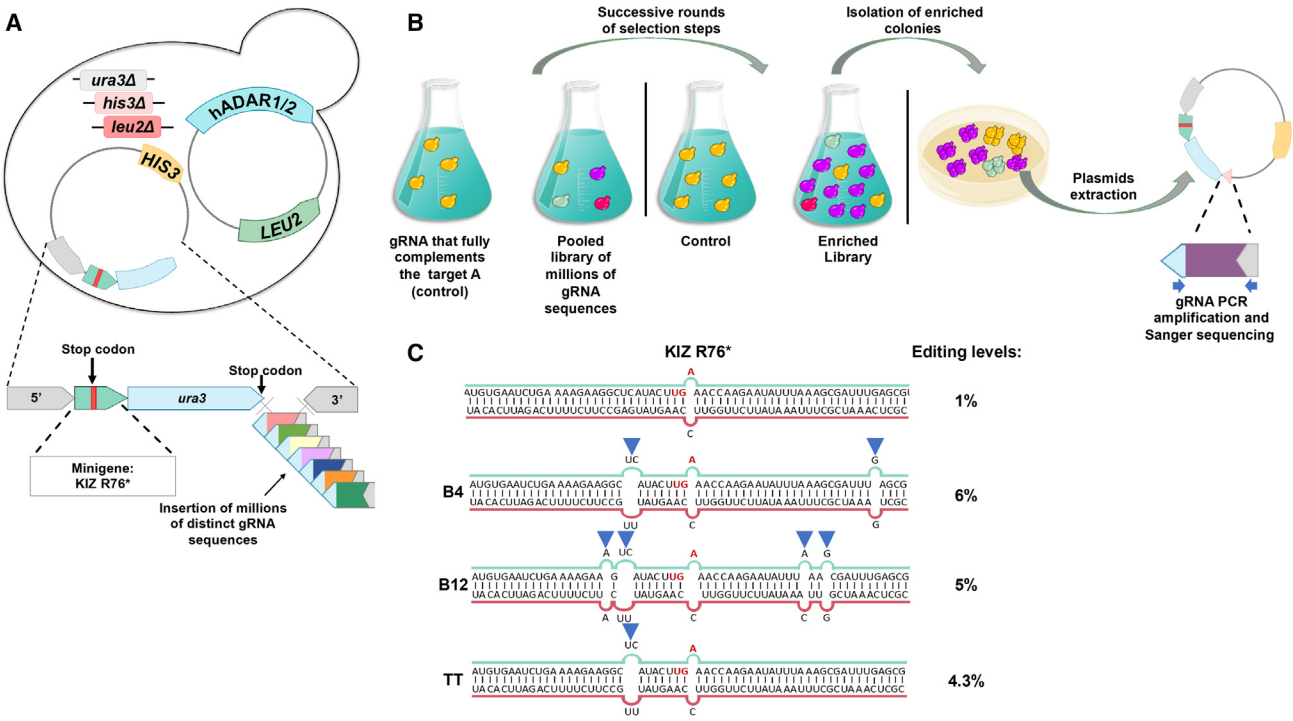

Figure 5. The high-throughput yeast-based screening system

(A) A library of approximately 10^7 yeast strains, described in Figure 2, was created by using *in vivo* homologous recombination to insert distinct gRNA sequences at the 5′ end of the reporter gene. (B) The process of selecting improved gRNA variants targeting the KIZ R67* mutation. The sample containing yeast strains with a gRNA that forms perfect dsRNA structures with the target mutation was used as a baseline growth control and compared with the pooled library. After iterative rounds of enrichment in a medium lacking uracil, we serially diluted a sample from the enriched library and plated single cells on a medium that selects for the *HIS3* plasmid that harbors the gRNAs. Plasmids were prepared from the developing colonies, and the sequences of the gRNAs that facilitated growth in the selected colonies were determined through Sanger sequencing of the PCR products, using universal primers flanking the insertion sites of the gRNA-encoding DNA (blue arrows). (C) Sequence of the target adenosine and flanking sequence (green) and the complementary identified gRNAs (red) (termed "B4", "B12", and "TT") compared with the control dsRNA containing a single A-C mismatch at the target adenosine. The editing levels of the control were determined using NGS as described above.

editing levels approaching 66% in Sanger sequencing (Table 1; Figures 6C and 6D).

Editing was also observed in cells transfected with a minigene reporter construct containing the nonsense *USH2A* mutation (c.11864G>A, p.W3955*) and in this case the target adenosine for editing is the mutation itself, for a complete correction of the mutation (Table 1). Because of high levels of editing in the yeast model for both *USH2A* gRNAs with and without the GR motif, we tested each in the reporter system. Higher levels of editing were noticed in ADAR1 p.110-overexpressing and ADAR2-overexpressing HeLa cells transfected with a USH2A 60-mer gRNA without an GR motif compared with the levels observed in the samples transfected with the GR motif in which no editing was apparent in the ADAR1 p.110-overexpressing HeLa cells (Table 1; Figure S6). Both mCherry and EGFP expression were observed for all samples transfected with both types of gRNA.

Highest editing was seen in both ADAR1 p.110 and ADAR2 cells treated with the *USH2A* gRNA without the GR motif. For samples where RNA editing was observed, an average of 30.0% (n = 3) and 31.2% (n = 5) editing was observed in Sanger sequencing and NGS, respectively, for ADAR1 p.110-expressing cells compared with an average of 29.5% (n = 5) and 20.5% (n = 4) in ADAR2-expressing HeLa cells (Table 1). For samples transfected with *USH2A* gRNAs with an GR motif, the only levels of editing noted were in ADAR2-expressing HeLa cells with an average of 10.4% (n = 4) and 9% (n = 4) editing in Sanger sequencing and NGS, respectively (Table 1).

Both minigene reporter constructs containing nonsense mutations in the *FAM161A* gene (c.880A>T, p.K294*) and *KIZ* gene (c.226C>T, p.R76*) were less amenable to ADAR editing, probably because of a neighboring guanosine, 5′ to the target adenosine, previously described as being challenging to edit due hinderance of necessary base flipping for deamination.[28] Cell lines transfected with the mutant *FAM161A* gene fragment-containing reporter construct and treated with the 60-mer gRNA showed an average editing of 1.7% (n = 2) and 2.5% (n = 2) in Sanger sequencing and NGS, respectively, in ADAR1-overexpressing HeLa cells compared with 5.2% (n = 2) and 4.7% (n = 2) for ADAR2-overexpressing HeLa cells (Table 1). EGFP fluorescence was noted in some of the wells (Figure S4).

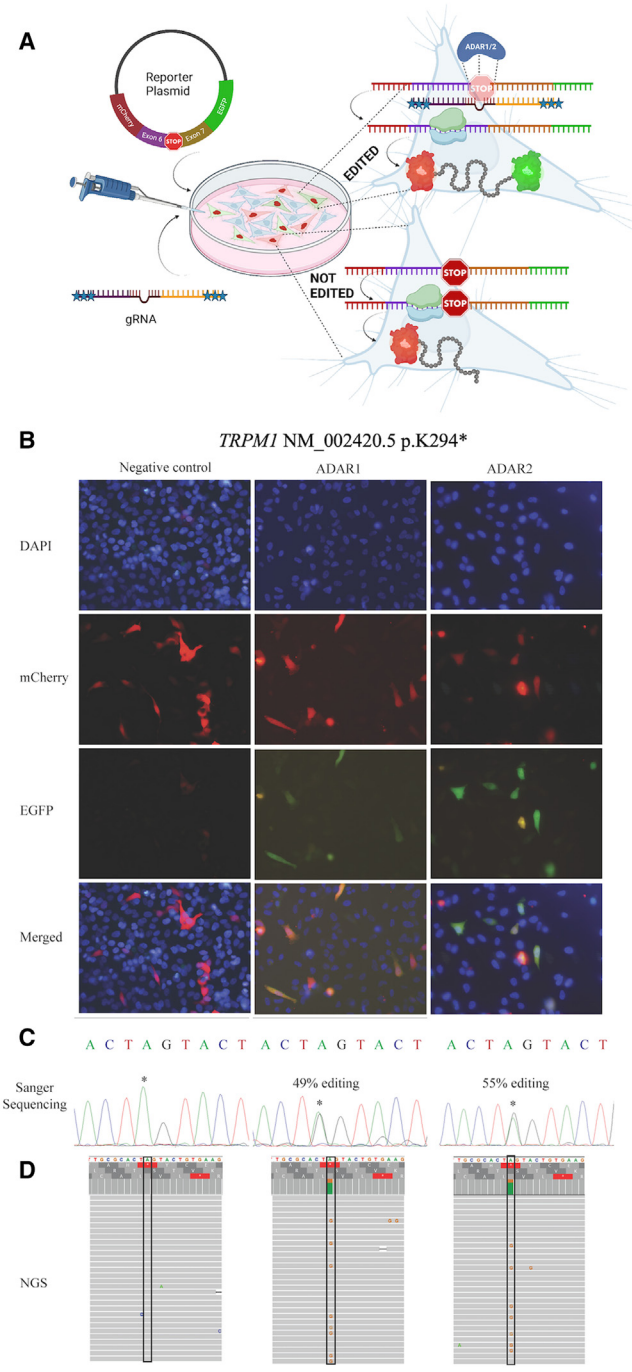

Figure 6. RNA editing in HeLa cells

Representative images from samples of ADAR1 p.110 (ADAR1)-overexpressing and ADAR2-overexpressing HeLa cells transfected with both the *TRPM1* nonsense mutation reporter plasmid and 60-mer chemically modified gRNA at 96 h post-seeding. (A) Schematic of the in-*vitro* experiment. (B) Fluorescent microscopy. (C) Sanger sequence. (D) Next-generation sequencing reads in IGV viewer.

Targeted editing of RNA transcribed from the *KIZ* reporter construct proved challenging as well. Among ADAR1-expressing HeLa cells treated with the KIZ gene fragment-containing reporter construct and 60-mer gRNA, where RNA editing was observed, an average of 3.3% (n = 2) and 7.4% (n = 6) of target adenosine editing was measured in Sanger sequencing and NGS, respectively, while an average of 9.9% (n = 3) and 7.8% (n = 6) editing was measured in ADAR2-expressing treated HeLa cells (Table 1). The same mammalian reporter system expressing ADAR2 was used to test the editing efficiency of the three library-identified gRNAs "B4," "B12," and "TT" (Figure 5C) complementary to the *KIZ* target with identified mismatches. One of the three tested gRNAs ("TT") showed a 1.4× increase in editing compared with the original gRNA (Figure S7).

Off-target editing levels are also sequence dependent

A collateral consequence of using endogenous ADAR for RNA editing can be off-target editing affecting neighboring adenosines. Just as the editing levels of the RNA differed on the basis of gene and mutation, so too did the resulting off-target editing levels (Figure 7). *TRPM1* has 16 potential off-target sites within the complementary region, 4 of them have a G 5′ nucleotide neighbor to the A and were unperturbed in both ADAR1 p.110-overexpressing and ADAR2-overexpressing samples, with only 2 sites and 5 sites showing levels of editing more than 2× background respectively, with an average of 1.1% and 2.9% for the adenosines that were edited (corrected for background). Each off-target adenosine that was edited would cause an amino acid change in that particular transcript. *KIZ* had the highest levels of off-target editing, while *FAM161A* and *TRPM1* had almost none and minimal off-target editing, respectively. *USH2A* has 17 potential off-target sites; 7 are upstream to the target and 10 downstream. Only 3 sites show significant levels of editing with a maximum of 13%, 7 nt downstream to the target when the target averaged 29% editing. Moreover, when analyzing the off-target effects of the data obtained in yeast and comparing the two gRNAs used for the *USH2A* and *TRPM1* variants (60nt-SpD or 30nt-SpD-GR), we observed that in the case of *USH2A* and hADAR1, no off-targets were detected. Interestingly, the total number of off-target sites was reduced from 4 to 2 when using 60nt-SpD and 30nt-SpD-GR respectively. Furthermore, no significant editing was detected in *TRPM1* in the presence of these gRNAs and hADAR2. However, in cells expressing hADAR1, a similar effect was detected, resulting in a reduction in the total number of off-target sites from 4 to 0 (see Figure S8). These results imply that in addition to the previously described approaches,[29–32] generally, shorter gRNAs can be used to reduce bystander editing. However, it may come with a cost, as in both cases, the RNA-editing efficiency of the target adenosine was negatively affected.

DISCUSSION

IRDs are a set of devastating diseases that can cause blindness, with at least 5.5 million individuals affected worldwide.[16] As the injured photoreceptors cannot regenerate, curing retinal degeneration is an extremely challenging task. Indeed, of the many therapeutic modalities developed and preclinically tested, there is currently only one US Food and Drug Administration (FDA)-approved treatment, namely, AAV-based gene

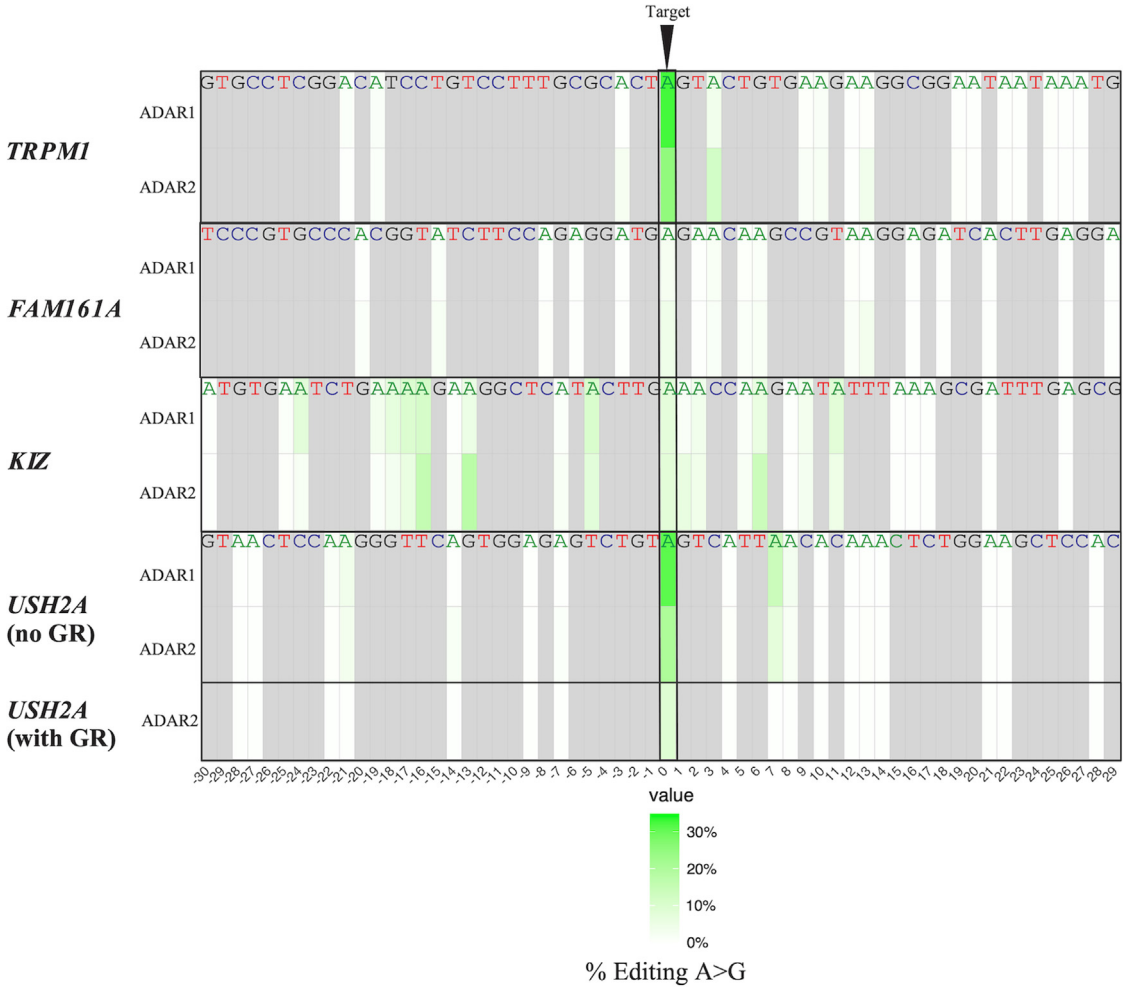

Figure 7. Heatmap of average off-target and on-target editing rate for adenosines in complementarity region

Average editing level percentages are shown for *TRPM1* (n = 8, n = 10), *KIZ* (n = 2, n = 2), *FAM161A* (n = 2, n = 2), and *USH2A* (without R/G) (n = 2, n = 2) in ADAR1 p.110-overexpressing and ADAR2-overexpressing HeLa cells, and *USH2A* (with GR) in ADAR2-overexpressing HeLa cells, corrected for NGS sequencing noise. Positions below the heatmap are relative to the target adenosine (0), bases in gray are non-adenosine bases, and adenosines with 0% editing are white, gradually increasing to deep green in correlation with increasing editing levels.

therapy, which is suitable for but one of the 277 genes found to be mutated in the >50 IRD phenotypes. Here we propose a personalized approach for curing IRDs: applying RNA editing mediated by ADARs to target nonsense IRD mutations. Given that most adenosines are not likely to occur in a proper structure for editing, a main challenge is to design antisense gRNAs to artificially create an editable dsRNA structure around a user-defined target to redirect hADAR activity to this site. However, the rules for the construction of these elements are only partially known. To address this issue, we established for the first time a gRNA screening pipeline that is based on a powerful yeast-based initial screening system, followed by validation steps in a dual reporter system using HeLa cells which enables faster, easier, and cheaper approaches that can be tailored for the screening of a large number of candidate gRNAs to uncover those that are particularly more efficient in editing selected targets.

Yeast cells have been previously used as a model system to explore ADAR functionality and preferences. These studies have focused on hADARs and identified a novel set of editing substrates.[33,34] Furthermore, the co-expression of hADARs with selected substrates has allowed monitoring the effects of mutations within the ADAR domains or the target dsRNA structure on the editing levels.[35,36] These studies nicely demonstrated that ADAR enzymes can be expressed in yeast and carry out their biological function. Thus it was not surprising that the strains expressing the *KIZ*-p.R76* and *FAM161A* p.R523* mutations showed minimal growth and were difficult to edit. These mutants carry guanosines at the 5′ end of the target adenosine, which are largely depleted from the 5′ end of natively edited adenosines,[23] most probably because of a steric clash between the 2-amino group of the 5′ guanosine and G489 of ADAR2 loop involved in stabilizing the flipped-out conformation required for the adenosine deamination

reaction.[7] This concept is supported experimentally by a recent study,[26] as described in the control experiment outlined in Figure 4. By introducing a G:G mismatch at the 5′ end of the target adenosine, we observed a notable enhancement of editing, in line with the predictions made in this study that such mismatch should solve this steric problem.

This together with the clear correlation between the growth and editing levels in yeast and HeLa cells nicely demonstrate that the yeast-based screening system can be used as an efficient in-vitro platform for testing and optimizing selected "specificity domains" and recruitment elements. However, it is important to emphasize that the yeast system does not replicate the endogenous dsRNA structure surrounding the target adenosines. Furthermore, in addition to the ADARs' dsRBDs, the human genome encodes for more than 1,000 RNA-binding proteins (RBPs), 16 of which contain dsRBDs that may directly compete with ADAR binding depending on the cellular context.[37–39] Thus, it is crucial to highlight the significance of assessing and validating the results obtained in our yeast and HeLa cell pipeline in later stages, using model systems that mirror the endogenous dsRNA structure, and the dsRBP expression profile of the therapeutically relevant target cell.

Indeed, we have identified three gRNAs, termed "B4," "B12," and "TT," that exhibited enhanced activity in yeast. Interestingly, this enhancement was replicated in mammalian cells only for the "TT" gRNA. Considering the aforementioned possibilities, it is plausible that only the bulge present in "TT," a portion of which is also found in "B4" and "B12," plays a crucial role in editing activity. Moreover, it is conceivable that the additional bulges in "B4" and "B12" might actually hinder their performance in mammalian cells. This specific hypothesis will be further explored in our forthcoming studies.

The pipeline we describe here is suitable mainly for nonsense mutations and in rare cases might be adapted for other type of mutations by shifting the frame of the target sequence to create a nonsense mutation around the target "A" if is surrounded by TAA, TGA, or TAG. Nonsense mutations are responsible for 18% of IRD-causing mutations[11] and 11% of inherited diseases in humans,[40] leaving a relatively large number of mainly missense and splice-site mutations that cannot be studied using this pipeline. Therefore additional screening systems need to be developed aiming to identify the most efficient gRNAs for each mutation using genetic libraries as gRNAs.[41] Unlike the extremely large number of gRNAs that can be tested using the yeast screening tool described here, cloning-based libraries of gRNAs in human cells are limited by the number of studied inserts and therefore will allow only a more restricted analysis of missense and splice-site mutations.

The yeast model system described here is based on the dynamic range of the *URA3* reporter gene, which leads to a WT-like growth of treated mutations even with a low editing level of about 12% editing. This feature will not enable us to distinguish between gRNAs with very high efficiency (more than 50%) to those in the lower range of 20%–25% editing. To overcome this issue, we are currently screening for other auxotrophic markers or fluorophores that will serve as alternative reporter genes.

Three out of the four nonsense mutations we studied are amenable for RNA editing by recoding nonsense to a missense variant, while only the *USH2A* nonsense mutation can be fully corrected by ADAR RNA editing. This distribution reflects nonsense mutations in general and therefore one needs to verify that the newly coded amino acid variant is not pathogenic. As functional assessment of protein isoforms is usually limited and is currently not available for most disease-causing proteins, other measures need to be taken to decrease the chances for such risk. We therefore selected genes (*KIZ*, *FAM161A*, and *TRPM1*) with either null reported mutations only or with a limited number of reported missense mutations. The encoded proteins are therefore likely to tolerate missense changes. This can be further validated by functional rescue of the retinal phenotype in an appropriate knockin mouse model. Currently only one such model is available[42] for the *FAM161A* nonsense mutation. On the other hand, some of the major genes that cause retinal degeneration when mutated in humans do not cause a retinal phenotype in mouse models, therefore limiting the abilities of proving functional disease restoration.

One of the major concerns regarding nucleic acid manipulation as a therapeutic approach is the possibility of off-target effect and mainly non-targeted coding regions that might be edited by such manipulations.[43] Although this concern is mainly valid for DNA editing using externally augmented proteins, such as CRISPR-Cas9, that might cause permanent DNA sequence abnormalities, ADAR-based RNA editing can only create missense changes,[44,45] mainly in the vicinity of the targeted A, and not null mutations. In addition, RNA editing is temporary and can be tuned at any stage. Here we performed an off-target analysis of the gRNA region and show that once editing of the target "A" is efficient, off-targets are rare with extremely limited levels. On the other hand, if the target "A" shows limited editing levels, other "A"s in its vicinity might undergo relatively high editing. Our data also show that for both target and non-target "A"s, similar rules might apply and the editing of both might be low if the "A" is preceded by a "G" nucleotide. This is only one example of challenging sequences for editing and recent studies that are based on sequence libraries unravel potential sequence modifications that might overcome these challenges.[41]

The systems used in the present study use artificially expressed ADAR in both yeast and HeLa cell lines. Moving toward therapeutic options will require either recruiting endogenous ADAR or using AAV to deliver an exogenous ADAR to retinal cells. It is therefore difficult to predict how well the results obtained in the present study will be translated into editing levels *in vivo*. However, as the expression levels of ADAR2 in neurons generally, and in retinal cells particularly, are relatively high, one may hypothesize that RNA editing in photoreceptor cells will reach the required level to stop disease progression.

In summary, we describe here a pipeline for efficient design of gRNAs for RNA editing of IRD mutations. Together with previous preliminary studies,[46,47] we provide here proof of concept that RNA editing

might serve as an excellent therapeutic tool for genetic diseases. The next major challenge would be to obtain meaningful RNA editing levels in retinal cells using endogenous ADAR enzymes.

MATERIALS AND METHODS

Yeast strains

All the strains used in this study are isogenic to the diploid strain BY4743 (*MAT*a/α *ura3*Δ*0*/*ura3*Δ*0 leu2*Δ*0*/*leu2*Δ*0 his3*Δ*1*/*his3*Δ*1 lys2*Δ*0*/*LYS2 met15*Δ*0*/*MET15*.[48]

The relevant genotypes are presented in Table S1.

Yeast plasmids

The relevant plasmids used in this study are presented in Table S1. The Gateway recombination cloning technology (Invitrogen, Waltham, MA) was used to clone the hADAR2 into the *URA3* marked plasmid (pYES2-DEST52 Gateway destination vector [catalog #12286-019]; Thermo Fisher Scientific, Waltham, MA). The *URA3* marker was later swapped with the *LEU2* marker to create BSB641. This plasmid enables the conditional expression of the hADARs in yeast, under a galactose-inducible promoter (*GAL1*p-hADAR2).

The plasmid carrying the *URA3* reporter gene (BSB656) was created using *in vivo* homologous recombination in yeast, by co-transforming the yeast *URA3* gene (including its 5′ promoter region and 3′ UTR) into a linearized *HIS3*-marked plasmid (pRS313[49]) digested with XhoI/XbaI. *In vivo* homologous recombination was used to insert the target and reverse complement "tail" sequences (shown in Table S2) by linearizing BSB656 with either *Eco*RI (target insertion) or *Bam*HI ("tail" insertion). Site-directed mutagenesis was used to insert the *Eco*RI (right before the *URA3* start codon) and *Bam*HI (right after the *URA3* stop codon). The target and "tail" insertions were validated by PCR and Sanger sequence using OSB2366/OSB207 and OSB1202/OSB502, respectively (Table S3).

Yeast growth conditions

Yeast cells were grown in synthetic complete medium (SC; 0.17% yeast nitrogen base, 0.5% $(NH_4)_2SO_4$, and amino acids), supplemented with either 2% glucose (SD), raffinose (SC+Raf), or galactose (SC+Gal), and 0.2% of either (-Histidine-Leucine) or (-Histidine-Leucine-Uracil) amino acid mix. Unless otherwise stated, cells were grown at 30°C. For logarithmic culture, cells were grown for 16–18 h and then back diluted 10× with fresh media and allowed to grow for the indicated time.

Yeast cell growth assays

To measure cells viability, exponentially growing cells were normalized to a density of 1×10^6 cells/mL into a 96-well plate containing selective medium supplemented with galactose to induce hADAR genes expression and incubated for 24 h at 30°C while shaking. Cell growth was then determined by measuring the absorbance at 600 nm in 30 min intervals using a Tecan Spark 10M multimode microplate reader. The area under the curve (AUC) was calculated using the Growthcurver package in R.

Yeast NGS

RNA samples were extracted from yeast cells using the MasterPure Yeast RNA purification Kit (Epicentre Technologies, Madison, WI). cDNA was synthesized using ProtoScript II Reverse transcriptase (OSB2798; NEB, Ipswich, MA). Then the IRD fragments were amplified using 15 PCR cycles, with specific primers for the relevant region (forward primers OSB2795-7 and OBS2840) and universal reverse primer (OSB2798). The primers included an overhang partial adapter for the UD indexes (sp p5 and sp p7). Adapters for Illumina NGS were added by 8 PCR cycles using the IDT for Illumina UD indexes. PCR products were then cleaned using KAPA pure beads in a 1:1 ratio, followed by DNA quantification and quality check using Qubit and tapestation, respectively. Finally, the samples were subjected to NGS by Illumina sequencing.

Library of gRNA construction and screening process

A library of random gRNA sequences was created using single-stranded DNA primers ordered from Integrated DNA Technologies (IDT). PCR amplification was performed using universal primers flanking the random sequences (OSB2874+2875). The resulting DNA fragments were co-transformed with a BamHI-digested plasmid containing the selected minigene into a strain carrying the hADAR2 plasmid. This step resulted in the integration of the PCR fragment at the 3′ UTR of the URA3 reporter gene through *in vivo* homologous recombination. The resulting yeast transformants, each carrying a unique gRNA, were pooled together and subjected to successive rounds of selection steps under uracil starvation in the presence of galactose (SC+GAL-HIS-LEU-URA). Next, to identify the gRNA sequences responsible for enhancing editing and stimulating induced growth of cells in the pooled culture, we serially diluted a sample from the library and plated single cells on a medium that selects for the plasmid harboring the gRNAs and hADAR2 (SD-HIS-LEU). Plasmids harboring the gRNAs that facilitated growth in the selected colonies were determined through Sanger sequencing of the PCR products, using universal primers flanking the insertion sites of the gRNA-encoding DNA (OSB502 and 1202).

Stable ADAR1 p.110-expressing and ADAR2-expressing HeLa cell line

HeLa cells conditionally overexpressing ADAR1 or ADAR2 were created using a CRISPR-CAS9-mediated system for the insertion of a doxycycline (Dox)-induced ADAR1 and ADAR2 cassette into the AAVS1 locus in HeLa cells.[50]

Reporter plasmids

An insert (ranging in size from 152 to 233 nt) harboring a cDNA fragment flanking the four studied mutations (*TRPM1*: c.880A>T, p.K294*; *FAM161A*: c.1567C>T, p.R523*; *KIZ*: c.226C>T, p.R76*; *USH2A*: c.11864G>A, p.W3955*) was cloned into the reporter plasmid expressing mCherry and EGFP (#86639; Addgene, Watertown, MA) in frame with the fluorescent proteins. Cloning was performed using restriction enzymes *Kpn*I (#00914286; Thermo Fisher Scientific) and *Bam*HI-HF (#R3136; New England Biolabs, Ipswich, MA) and subsequently ligated and transformed into

DH5α-HIT-competent cells (#RH618; RBC, New Taipei City, Taiwan). Plasmids were purified using a plasmid purification kit (QIAprep Spin Miniprep Kit [#2714]; Qiagen, Hilden, Germany). Sequences of the cloned products were verified using Sanger sequencing.

gRNA generation

The chemically modified 73-mer gRNA (4 nmol) with an 18-nt-long complementarity region and a 55 nt GR motif tail targeting the specific adenosine in GAPDH cloned into the reporter plasmid was ordered from Biospring (Frankfurt, Germany) as previously described by Merkle et al.[27] for the validation of the reporter system.

All chemically modified gRNAs used for the editing of IRD mutations were purchased as high-performance liquid chromatography (HPLC)-cleaned, 60-mer RNAs at a 4–6 nmol scale from Biospring. Both the 5′ and 3′ ends of the gRNA contained three 2′ O-methyl bases and two phosphorothioate bonds. All bases were complementary to the target sequence except for the thirtieth base, to be directly across from the target adenosine, which was a cytosine, creating a cytosine-adenosine mismatch (sequences are shown in Table S4).

In vitro editing in HeLa cells

Editing assays were performed with the stable ADAR-overexpressing HeLa cell line under transient expression controlled by the introduction of Dox, reporter plasmids, and chemically modified 60-mer gRNAs.

HeLa cells were cultured in DMEM + 10% fetal bovine serum (FBS) + 1% penicillin/streptomycin (P/S) (100 U/mL penicillin and 100 μg/mL streptomycin) + 1% L-glutamine. For editing, 4.0×10^4 of either ADAR1 p.110-expressing or ADAR2-expressing HeLa cells were seeded into 24-well plates in 500 μL DMEM + 10% FBS + 1% P/S (100 U/mL penicillin and 100 μg/mL streptomycin) + 1% L-glutamine + 1 ng/mL Dox. After 24 h, medium and Dox was changed and the reporter plasmid was transfected into each well; 50 μL Opti-MEM I Reduced-Serum Medium was mixed with 0.5 μg plasmid DNA and 1.0 μL TransfeX (AATC, Atlanta, GA) reagent, incubated at room temperature for fifteen minutes, and then distributed dropwise to each well. After 48 h, medium and Dox was changed, and the gRNA was transfected into each well; 1.5 μL Lipofectamine RNAiMAX (Thermo Fisher Scientific) and 25 pmol gRNA were each diluted in a total volume of 50 μL OptiMEM. After each solution was incubated for five minutes, the two solutions were combined, and after another 20 min incubation, the 100 μL transfection mix was evenly distributed into each well. After 72 h, the cells seeded on 10 mm coverslips were fixated using 4% paraformaldehyde (PFA) and mounted onto slides using DAPI mounting solution or harvested for RNA isolation using the Quick-RNA Miniprep Kit (Zymo Research, Irvine, CA) and Sanger sequencing as well as NGS.

Off-target analysis of NGS data

Binary alignment map (BAM) files were created by aligning the corresponding FASTQ files to a manually generated fasta file containing the insert sequence using bowtie2 (https://usegalaxy.org). Simultaneous analysis of NGS-generated samples was done using an RStudio code with BAM files used as input and nucleotide count at each reference sequence adenosine position as output. For each off-target site, the percentage of A-G in the negative control was deducted from the corresponding value in each sample, followed by heatmap generation.

DATA AND CODE AVAILABILITY

All data are available by request.

SUPPLEMENTAL INFORMATION

Supplemental information can be found online at https://doi.org/10.1016/j.omtn.2024.102130.

ACKNOWLEDGMENTS

This work was supported by the Israel Science Foundation (grant 1778/20), the Foundation Fighting Blindness (grants TA-GT-0620-0790-HUJ and PPA-0923-0865-HUJ to S.B.-A., E.B., E.Y.L., and D.S.), and the STEP- GTP fellowship and the Ariane de Rothschild Women Doctoral Program (to N.S.). E.Y.L. was supported by grants from the Israeli Ministry of Science (grant 3-17916) and by the Israel Science Foundation (grant 2039/20 and 2637/23).

AUTHOR CONTRIBUTIONS

Conceptualization, N.S., R.S., A.B.D., J.V., E.B., E.Y.L., D.S., and S.B.-A.; data curation, N.S., R.S., A.B.D., and J.V.; formal analysis, N.S., R.S., A.B.D., and J.V.; funding acquisition, E.B., E.Y.L., D.S., and S.B.-A.; investigation, N.S., R.S., A.B.D., and J.V.; methodology, D.S. and S.B.-A.; software, J.V. and Z.R.; supervision, E.B., E.Y.L., D.S., and S.B.-A.; visualization, N.S., R.S., A.B.D., J.V., Z.R., D.S., and S.B.-A.; writing – original draft, N.S., R.S., S.B.-A., and D.S.; writing – review & editing, N.S., R.S., A.B.D., J.V., E.B., E.Y.L., D.S., and S.B.-A.

DECLARATION OF INTERESTS

S.B.-A. and E.Y.L. are inventors of a filed patent based on the work published here: "Composition and Methods for Identifying Antisense Guide RNA for RNA Editing" (7632-PCT | PCT/IL2021/050800, Bar-Ilan University).

REFERENCES

1. Bazak, L., Haviv, A., Barak, M., Jacob-Hirsch, J., Deng, P., Zhang, R., Isaacs, F.J., Rechavi, G., Li, J.B., Eisenberg, E., and Levanon, E.Y. (2014). A-to-I RNA editing occurs at over a hundred million genomic sites, located in a majority of human genes. Genome Res. *24*, 365–376. https://doi.org/10.1101/gr.164749.113.

2. Licht, K., Hartl, M., Amman, F., Anrather, D., Janisiw, M.P., and Jantsch, M.F. (2019). Inosine induces context-dependent recoding and translational stalling. Nucleic Acids Res. *47*, 3–14. https://doi.org/10.1093/nar/gky1163.

3. Bass, B.L. (2002). RNA Editing by Adenosine Deaminases That Act on RNA. Annu. Rev. Biochem. *71*, 817–846. https://doi.org/10.1146/annurev.biochem.71.110601.135501.

4. Eisenberg, E., and Levanon, E.Y. (2018). A-to-I RNA editing - Immune protector and transcriptome diversifier. Nat. Rev. Genet. *19*, 473–490. https://doi.org/10.1038/s41576-018-0006-1.

5. Porath, H.T., Schaffer, A.A., Kaniewska, P., Alon, S., Eisenberg, E., Rosenthal, J., Levanon, E.Y., and Levy, O. (2017). A-to-I RNA Editing in the Earliest-Diverging Eumetazoan Phyla. Mol. Biol. Evol. *34*, 1890–1901. https://doi.org/10.1093/molbev/msx125.

6. Savva, Y.A., Rieder, L.E., and Reenan, R.A. (2012). The ADAR protein family. Genome Biol. *13*, 252. https://doi.org/10.1186/gb-2012-13-12-252.

7. Matthews, M.M., Thomas, J.M., Zheng, Y., Tran, K., Phelps, K.J., Scott, A.I., Havel, J., Fisher, A.J., and Beal, P.A. (2016). Structures of human ADAR2 bound to dsRNA reveal base-flipping mechanism and basis for site selectivity. Nat. Struct. Mol. Biol. *23*, 426–433. https://doi.org/10.1038/nsmb.3203.

8. Polson, A.G., Bass, B.L., and Casey, J.L. (1996). RNA editing of hepatitis delta virus antigenome by dsRNA-adenosine deaminase. Nature *380*, 454–456. https://doi.org/10.1038/380454a0.

9. Meisel, R. (2021). CRISPR-Cas9 Gene Editing for Sickle Cell Disease and β-Thalassemia. N. Engl. J. Med. *384*, e91. https://doi.org/10.1056/NEJMc2103481.

10. Gillmore, J.D., Maitland, M.L., and Lebwohl, D. (2021). CRISPR-Cas9 In Vivo Gene Editing for Transthyretin Amyloidosis. N. Engl. J. Med. *385*, 1722–1723. https://doi.org/10.1056/NEJMc2114592.

11. Buchumenski, I., Roth, S.H., Kopel, E., Katsman, E., Feiglin, A., Levanon, E.Y., and Eisenberg, E. (2021). Global quantification exposes abundant low-level off-target activity by base editors. Genome Res. *31*, 2354–2361. https://doi.org/10.1101/gr.275770.121.

12. Gold, A., Levanon, E.Y., and Eisenberg, E. (2021). The New RNA-Editing Era - Ethical Considerations. Trends Genet. *37*, 685–687. https://doi.org/10.1016/j.tig.2021.04.013.

13. Xiang, Y., Katrekar, D., and Mali, P. (2022). Methods for recruiting endogenous and exogenous ADAR enzymes for site-specific RNA editing. Methods *205*, 158–166. https://doi.org/10.1016/j.ymeth.2022.06.011.

14. Pfeiffer, L.S., and Stafforst, T. (2023). Precision RNA base editing with engineered and endogenous effectors. Nat. Biotechnol. *41*, 1526–1542. https://doi.org/10.1038/s41587-023-01927-0.

15. Schneider, N., Sundaresan, Y., Gopalakrishnan, P., Beryozkin, A., Hanany, M., Levanon, E.Y., Banin, E., Ben-Aroya, S., and Sharon, D. (2022). Inherited retinal diseases: Linking genes, disease-causing variants, and relevant therapeutic modalities. Prog. Retin. Eye Res. *89*, 101029. https://doi.org/10.1016/j.preteyeres.2021.101029.

16. Hanany, M., Rivolta, C., and Sharon, D. (2020). Worldwide carrier frequency and genetic prevalence of autosomal recessive inherited retinal diseases. Proc. Natl. Acad. Sci. USA *117*, 2710–2716. https://doi.org/10.1073/pnas.1913179117.

17. Rivolta, C., Sharon, D., DeAngelis, M.M., and Dryja, T.P. (2002). Retinitis pigmentosa and allied diseases: numerous diseases, genes, and inheritance patterns. Hum. Mol. Genet. *11*, 1219–1227.

18. Pinelli, M., Carissimo, A., Cutillo, L., Lai, C.-H., Mutarelli, M., Moretti, M.N., Singh, M.V., Karali, M., Carrella, D., Pizzo, M., et al. (2016). An atlas of gene expression and gene co-regulation in the human retina. Nucleic Acids Res. *44*, 5773–5784. https://doi.org/10.1093/nar/gkw486.

19. Hajji, K., Sedmík, J., Cherian, A., Amoruso, D., Keegan, L.P., and O'Connell, M.A. (2022). ADAR2 enzymes: efficient site-specific RNA editors with gene therapy aspirations. RNA *28*, 1281–1297. https://doi.org/10.1261/rna.079266.122.

20. Chalk, A.M., Taylor, S., Heraud-Farlow, J.E., and Walkley, C.R. (2019). The majority of A-to-I RNA editing is not required for mammalian homeostasis. Genome Biol. *20*, 268. https://doi.org/10.1186/s13059-019-1873-2.

21. Tan, M.H., Li, Q., Shanmugam, R., Piskol, R., Kohler, J., Young, A.N., Liu, K.I., Zhang, R., Ramaswami, G., Ariyoshi, K., et al. (2017). Dynamic landscape and regulation of RNA editing in mammals. Nature *550*, 249–254. https://doi.org/10.1038/nature24041.

22. Levanon, E.Y., Eisenberg, E., Yelin, R., Nemzer, S., Hallegger, M., Shemesh, R., Fligelman, Z.Y., Shoshan, A., Pollock, S.R., Sztybel, D., et al. (2004). Systematic identification of abundant A-to-I editing sites in the human transcriptome. Nat. Biotechnol. *22*, 1001–1005. https://doi.org/10.1038/NBT996.

23. Eggington, J.M., Greene, T., and Bass, B.L. (2011). Predicting sites of ADAR editing in double-stranded RNA. Nat. Commun. *2*, 319. https://doi.org/10.1038/ncomms1324.

24. Lehmann, K.A., and Bass, B.L. (1999). The importance of internal loops within RNA substrates of ADAR1. J. Mol. Biol. *291*, 1–13. https://doi.org/10.1006/jmbi.1999.2914.

25. Harvey, S.C., Köster, A., Yu, H., Skolnick, P., Baumbarger, P., and Nisenbaum, E.S. (2001). AMPA receptor function is altered in GLUR2-deficient mice. J. Mol. Neurosci. *17*, 35–43. https://doi.org/10.1385/JMN:17:1:35.

26. Doherty, E.E., Karki, A., Wilcox, X.E., Mendoza, H.G., Manjunath, A., Matos, V.J., Fisher, A.J., and Beal, P.A. (2022). ADAR activation by inducing a syn conformation at guanosine adjacent to an editing site. Nucleic Acids Res. *50*, 10857–10868. https://doi.org/10.1093/nar/gkac897.

27. Merkle, T., Merz, S., Reautschnig, P., Blaha, A., Li, Q., Vogel, P., Wettengel, J., Li, J.B., and Stafforst, T. (2019). Precise RNA editing by recruiting endogenous ADARs with antisense oligonucleotides. Nat. Biotechnol. *37*, 133–138. https://doi.org/10.1038/s41587-019-0013-6.

28. Schneider, M.F., Wettengel, J., Hoffmann, P.C., and Stafforst, T. (2014). Optimal guideRNAs for re-directing deaminase activity of hADAR1 and hADAR2 in trans. Nucleic Acids Res. *42*, e87. https://doi.org/10.1093/nar/gku272.

29. Reautschnig, P., Wahn, N., Wettengel, J., Schulz, A.E., Latifi, N., Vogel, P., Kang, T.-W., Pfeiffer, L.S., Zarges, C., Naumann, U., et al. (2022). CLUSTER guide RNAs enable precise and efficient RNA editing with endogenous ADAR enzymes *in vivo*. Nat. Biotechnol. *40*, 759–768. https://doi.org/10.1038/s41587-021-01105-0.

30. Katrekar, D., Yen, J., Xiang, Y., Saha, A., Meluzzi, D., Savva, Y., and Mali, P. (2022). Efficient *in vitro* and *in vivo* RNA editing via recruitment of endogenous ADARs using circular guide RNAs. Nat. Biotechnol. *40*, 938–945. https://doi.org/10.1038/s41587-021-01171-4.

31. Qu, L., Yi, Z., Zhu, S., Wang, C., Cao, Z., Zhou, Z., Yuan, P., Yu, Y., Tian, F., Liu, Z., et al. (2019). Programmable RNA editing by recruiting endogenous ADAR using engineered RNAs. Nat. Biotechnol. *37*, 1059–1069. https://doi.org/10.1038/s41587-019-0178-z.

32. Yi, Z., Qu, L., Tang, H., Liu, Z., Liu, Y., Tian, F., Wang, C., Zhang, X., Feng, Z., Yu, Y., et al. (2022). Engineered circular ADAR-recruiting RNAs increase the efficiency and fidelity of RNA editing *in vitro* and *in vivo*. Nat. Biotechnol. *40*, 946–955. https://doi.org/10.1038/s41587-021-01180-3.

33. Eifler, T., Pokharel, S., and Beal, P.A. (2013). RNA-Seq analysis identifies a novel set of editing substrates for human ADAR2 present in Saccharomyces cerevisiae. Biochemistry *52*, 7857–7869. https://doi.org/10.1021/bi4006539.

34. Avram-Shperling, A., Kopel, E., Twersky, I., Gabay, O., Ben-David, A., Karako-Lampert, S., Rosenthal, J.J.C., Levanon, E.Y., Eisenberg, E., and Ben-Aroya, S. (2023). Identification of exceptionally potent adenosine deaminases RNA editors from high body temperature organisms. PLoS Genet. *19*, e1010661. https://doi.org/10.1371/journal.pgen.1010661.

35. Wang, Y., Havel, J., and Beal, P.A. (2015). A Phenotypic Screen for Functional Mutants of Human Adenosine Deaminase Acting on RNA 1. ACS Chem. Biol. *10*, 2512–2519. https://doi.org/10.1021/acschembio.5b00711.

36. Wang, Y., and Beal, P.A. (2016). Probing RNA recognition by human ADAR2 using a high-throughput mutagenesis method. Nucleic Acids Res. *44*, 9872–9880. https://doi.org/10.1093/nar/gkw799.

37. Pfaller, C.K., Li, Z., George, C.X., and Samuel, C.E. (2011). Protein kinase PKR and RNA adenosine deaminase ADAR1: new roles for old players as modulators of the interferon response. Curr. Opin. Immunol. *23*, 573–582. https://doi.org/10.1016/j.coi.2011.08.009.

38. Freund, E.C., Sapiro, A.L., Li, Q., Linder, S., Moresco, J.J., Yates, J.R., and Li, J.B. (2020). Unbiased Identification of trans Regulators of ADAR and A-to-I RNA Editing. Cell Rep. *31*, 107656. https://doi.org/10.1016/j.celrep.2020.107656.

39. Booth, B.J., Nourreddine, S., Katrekar, D., Savva, Y., Bose, D., Long, T.J., Huss, D.J., and Mali, P. (2023). RNA editing: Expanding the potential of RNA therapeutics. Mol. Ther. *31*, 1533–1549. https://doi.org/10.1016/j.ymthe.2023.01.005.

40. Mort, M., Ivanov, D., Cooper, D.N., and Chuzhanova, N.A. (2008). A meta-analysis of nonsense mutations causing human genetic disease. Hum. Mutat. *29*, 1037–1047. https://doi.org/10.1002/humu.20763.

41. Uzonyi, A., Nir, R., Shliefer, O., Stern-Ginossar, N., Antebi, Y., Stelzer, Y., Levanon, E.Y., and Schwartz, S. (2021). Deciphering the principles of the RNA editing code via large-scale systematic probing. Mol. Cell *81*, 2374–2387.e3. https://doi.org/10.1016/j.molcel.2021.03.024.

42. Matsevich, C., Gopalakrishnan, P., Obolensky, A., Banin, E., Sharon, D., and Beryozkin, A. (2023). Retinal Structure and Function in a Knock-in Mouse Model for the FAM161A-p.Arg523* Human Nonsense Pathogenic Variant. Ophthalmol. Sci. *3*, 100229. https://doi.org/10.1016/j.xops.2022.100229.

43. Wang, Y., Wang, M., Zheng, T., Hou, Y., Zhang, P., Tang, T., Wei, J., and Du, Q. (2020). Specificity profiling of CRISPR system reveals greatly enhanced off-target gene editing. Sci. Rep. *10*, 2269. https://doi.org/10.1038/s41598-020-58627-x.

44. Song, B., Shiromoto, Y., Minakuchi, M., and Nishikura, K. (2022). The role of RNA editing enzyme ADAR1 in human disease. Wiley Interdiscip. Rev. RNA *13*, e1665. https://doi.org/10.1002/wrna.1665.

45. Merkle, T., and Stafforst, T. (2021). New Frontiers for Site-Directed RNA Editing: Harnessing Endogenous ADARs. Methods Mol. Biol. *2181*, 331–349. https://doi.org/10.1007/978-1-0716-0787-9_19.

46. Kumar, S., Fry, L.E., Wang, J.H., Martin, K.R., Hewitt, A.W., Chen, F.K., and Liu, G.S. (2023). RNA-targeting strategies as a platform for ocular gene therapy. Prog. Retin. Eye Res. *92*, 101110. https://doi.org/10.1016/j.preteyeres.2022.101110.

47. Fry, L.E., Peddle, C.F., Barnard, A.R., McClements, M.E., and MacLaren, R.E. (2020). RNA Editing as a Therapeutic Approach for Retinal Gene Therapy Requiring Long Coding Sequences. Int. J. Mol. Sci. *21*, 777. https://doi.org/10.3390/ijms21030777.

48. Brachmann, C.B., Davies, A., Cost, G.J., Caputo, E., Li, J., Hieter, P., and Boeke, J.D. (1998). Designer deletion strains derived from Saccharomyces cerevisiae S288C: a useful set of strains and plasmids for PCR-mediated gene disruption and other applications. Yeast *14*, 115–132. https://doi.org/10.1002/(SICI)1097-0061(19980130)14:2<115::AID-YEA204>3.0.CO;2-2.

49. Sikorski, R.S., and Hieter, P. (1989). A system of shuttle vectors and yeast host strains designed for efficient manipulation of DNA in Saccharomyces cerevisiae. Genetics *122*, 19–27. https://doi.org/10.1093/genetics/122.1.19.

50. Qian, K., Huang, C.T.-L., Chen, H., Blackbourn, L.W., Chen, Y., Cao, J., Yao, L., Sauvey, C., Du, Z., and Zhang, S.-C. (2014). A simple and efficient system for regulating gene expression in human pluripotent stem cells and derivatives. Stem Cell. *32*, 1230–1238. https://doi.org/10.1002/stem.1653.

OMTN, Volume *35*

Supplemental information

A pipeline for identifying guide RNA sequences that promote RNA editing of nonsense mutations that cause inherited retinal diseases

Nina Schneider, Ricky Steinberg, Amit Ben-David, Johanna Valensi, Galit David-Kadoch, Zohar Rosenwasser, Eyal Banin, Erez Y. Levanon, Dror Sharon, and Shay Ben-Aroya

SUPPLEMENTAL METHODS

A. GAPDH 3' UTR insert: The 161 bp insert containing a portion of the 3' UTR of GAPDH, cloned into a reading frame in the pMcherry-EGFP reporter plasmid in which the editing of the target adenosine (blue) prevents translation termination, with a single base change of T>C (yellow) 8 bp downstream of the target adenosine to prevent a second stop codon in the reading frame.

CCCAGCAAGAGCACAAGAGGAAGAGAGAGACCCTCACTGCTGGGGAGTCCCTGCCA
CACTCAGTCCCCCACCACACTGAATCTCCCCTCCTCACAGTTGCCATGTAGACCCCT
CGAAGAGGGGAGGGGCCTAGGGAGCCGCACCTTGTCATGTACCATCAG

A- Target adenosine

C- T>C modification for prevention of stop codon

B. Chemically modified 73-mer gRNA development by the Stafforst group (1) used to edit a target adenosine in the 3' UTR of GAPDH cloned into the reported plasmid.

Key: (N)=RNA base, [N]=2'-OMe RNA base, *=Phosphorothioate linkage

Sequence for ssRNA (5'→3'):

[G*][G*][U](G)[U][C](GAGAAGAGGAGAA)[C](AA)[U](A)[U](G)[C][U](AAA)[U](G)[UU](G)[UUCUC](G)[UCUCCUC](G A)[C](A) [CCAGGGGU] (CCA) [CAUG][G*][C*][A*][A*][C]

1. Merkle,T., Merz,S., Reautschnig,P., Blaha,A., Li,Q., Vogel,P., Wettengel,J., Li,J.B. and Stafforst,T. (2019) Precise RNA editing by recruiting endogenous ADARs with antisense oligonucleotides. *Nat. Biotechnol.*, **37**, 133–138.

SUPPLEMENTAL TABLES:

Table S1-Yeast strains+plasmids.

YSB ID	Name	BSB ID	Plasmid A	BSB ID	Plasmid B
2907	pYEST-DEST52-hADAR2:LEU2 +FAM161A-R523W-URA3-BamHI:HIS3	641	pYEST-DEST52-hADAR2:LEU2	706	FAM161A-R523W-URA3-BamHI:HIS3
2911	pYEST-DEST52-hADAR2:LEU2 + TRPM1-K294W-URA3-BamHI:HIS3	641	pYEST-DEST52-hADAR2:LEU2	708	TRPM1-K294W-URA3-BamHI:HIS3
2988	pYEST-DEST52-hADAR2:LEU2 +FAM161A-p.R523*- ura3-31nt-GR(tail):HIS3	641	pYEST-DEST52-hADAR2:LEU2	731	FAM161A-p.R523*- ura3-31nt-GR(tail):HIS3
2989	pRS315::LEU2 +FAM161A-p.R523*- ura3-31nt-GR(tail):HIS3	61	pRS315::LEU2	731	FAM161A-p.R523*- ura3-31nt-GR(tail):HIS3
2990	pYEST-DEST52-hADAR2:LEU2 +TRPM1-p.K294*-ura3-30nt-GR(tail):HIS3	641	pYEST-DEST52-hADAR2:LEU2	732	TRPM1-p.K294*-ura3-30nt-GR(tail):HIS3
2991	pRS315::LEU2 +TRPM1-p.K294*-ura3-30nt-GR(tail):HIS3	61	pRS315::LEU2	732	TRPM1-p.K294*-ura3-30nt-GR(tail):HIS3
2992	pYEST-DEST52-hADAR2:LEU2 + KIZ-p.R76*-ura3-60nt(tail):HIS3	641	pYEST-DEST52-hADAR2:LEU2	727	KIZ-p.R76*-ura3-60nt(tail):HIS3
2993	pRS315:LEU2 + KIZ-p.R76*-ura3-60nt(tail):HIS3	61	pRS315:LEU2	727	KIZ-p.R76*-ura3-60nt(tail):HIS3
2994	pYEST-DEST52-hADAR2:LEU2 +TRPM1-p.K294*-ura3 60nt(tail):HIS3	641	pYEST-DEST52-hADAR2:LEU2	728	TRPM1-p.K294*-ura3-60nt(tail):HIS3
2995	pRS315::LEU2 +TRPM1-p.K294*-ura3-60nt (tail):HIS3	61	pRS315::LEU2	728	TRPM1-p.K294*-ura3-60nt(tail):HIS3
3003	pYEST-DEST52-hADAR2:LEU2 +FAM161A-p.R523*- ura3-60nt(tail):HIS3	641	pYEST-DEST52-hADAR2:LEU2	736	FAM161A-p.R523*- ura3-60nt(tail):HIS3
3004	pRS315::LEU2 +FAM161A-p.R523*- ura3-60nt(tail):HIS3	61	pRS315::LEU2	736	FAM161A-p.R523*- ura3-60nt(tail):HIS3
3005	pYEST-DEST52-hADAR2:LEU2 + KIZ-R76W-URA3-BamHI:HIS3	641	pYEST-DEST52-hADAR2:LEU2	704	KIZ-R76W-URA3-BamHI:HIS3
3054	pYEST-DEST52-hADAR2:LEU2 + KIZ-p.R76*-ura3-30nt-GR(tail):HIS3	641	pYEST-DEST52-hADAR2:LEU2	738	KIZ-p.R76*-ura3-30nt-GR(tail):HIS3
3055	pRS315::LEU2 + KIZ-p.R76*-ura3-30nt-GR:HIS3	61	pRS315::LEU2	738	KIZ-p.R76*-ura3-30nt-GR(tail):HIS3
3069	pYEST-DEST52-hADAR2:LEU2 + USH2A-p.W3955*-ura3-30nt-GR(tail):HIS3	641	pYEST-DEST52-hADAR2:LEU2	744	USH2A-p.W3955*-ura3-30nt-GR(tail):HIS3
3070	pRS315::LEU2 + USH2A-p.W3955*-ura3-30nt-GR(tail):HIS3	61	pRS315::LEU2	744	USH2A-p.W3955*-ura3-30nt-GR(tail):HIS3
3071	pYEST-DEST52-hADAR2:LEU2 + USH2A-p.W3955*-ura3-60nt:HIS3	641	pYEST-DEST52-hADAR2:LEU2	745	USH2A-p.W3955*-ura3-60nt:HIS3
3072	pRS315::LEU2 + USH2A-p.W3955*-ura3-60nt:HIS3	61	pRS315::LEU2	745	USH2A-p.W3955*-ura3-60nt:HIS3
3073	pYEST-DEST52-hADAR2:LEU2 + USH2A-W3955W-URA3:HIS3	641	pYEST-DEST52-hADAR2:LEU2	741	USH2A-W3955W-URA3:HIS3
3097	pYEST-DEST52-hADAR2:LEU2 + KIZ-p.R76*-ura3-60nt mismatches(tail):HIS3	641	pYEST-DEST52-hADAR2:LEU2	747	KIZ-p.R76*-ura3-60nt mismatches(tail):HIS3
3098	pRS315::LUE2 + KIZ-p.R76*-ura3-60nt mismatches(tail):HIS3	61	pRS315::LUE2	747	KIZ-p.R76*-ura3-60nt mismatches(tail):HIS3

3099	pYEST-DEST52-hADAR2:LEU2 +FAM161A-p.R523*- ura3-60nt mismatches (tail):HIS3	641	pYEST-DEST52-hADAR2:LEU2	748	FAM161A-p.R523*- ura3-60nt mismatches (tail):HIS3
3100	pRS315::LEU2 +FAM161A-p.R523*- ura3-60nt mismatches (tail):HIS3	61	pRS315::LEU2	748	FAM161A-p.R523*- ura3-60nt mismatches (tail):HIS3
3101	pYEST-DEST52-hADAR2:LEU2 +TRPM1-p.K294*-ura3 60nt mismatches(tail):HIS3	641	pYEST-DEST52-hADAR2:LEU2	749	TRPM1-p.K294*-ura3 60nt mismatches(tail):HIS3
3102	pRS315::LEU2 +TRPM1-p.K294*-ura3-60nt mismatches(tail):HIS3	61	pRS315::LEU2	749	TRPM1-p.K294*-ura3-60nt mismatches(tail):HIS3

Table S2-Target and Tails' sequence.

Name	Sequence
FAM161A-R523W	ATGAAATTGCCCAGTATTCTTAACCCAACTGCACAGAACAAAAACCTGCAGGAAACGAAGATAAATCatgCCTGTGCCTTGTAACTGCAACCCTCCCGTGCCCACGGTATCTTCCAGAGGATGGGAACAAGCCGTAAGGAGATCACTTGAGGAAAAGAAAATGTTGGAAGAAtcgaaagctacatataaggaacgtgctgctactcatcctagtcctgttgctgccaagctatttaata
FAM161A-p.R523*	ATGAAATTGCCCAGTATTCTTAACCCAACTGCACAGAACAAAAACCTGCAGGAAACGAAGATAAATCatgCCTGTGCCTTGTAACTGCAACCCTCCCGTGCCCACGGTATCTTCCAGAGGATGAGAACAAGCCGTAAGGAGATCACTTGAGGAAAAGAAAATGTTGGAAGAAtcgaaagctacatataaggaacgtgctgctactcatcctagtcctgttgctgccaagctatttaata
The 31nt+GR gRNA to the target FAM161A-p.R523*	gttacagaaaagcaggctgggaagcatatttgagaagatgcggccagcaaaactaaCTTACGGCTTGTTCcCATCCTCTGGAAGATAGGGTGGAATAGTATAACAATATGCTAAATGTTGTTATAGTATCCCACCTAAAACTGTATTATAAGTAAATGCATGTATACTAAACTCACAAA
The 60nt gRNA to the target FAM161A-p.R523*	caaagggaagggatgctaaggtagagggtgaacgttacagaaaagcaggctgggaagcatatttgagaagatgcggccagcaaaactaaTCCTCAAGTGATCTCCTTACGGCTTGTTCcCATCCTCTGGAAGATACCGTGGGCACGGGAAAAACTGTATTATAAGTAAATGCATGTATACTAAACTCACAAATTAGAGCTTCAATTTAATTATATCAGTTATTACCCGGGAATCTCGGTCGTAATGATT
The 60nt gRNA with mismatches to the target FAM161A-p.R523*	gaaaagcaggctgggaagcatatttgagaagatgcggccagcaaaactaaTCCTCAAGTGATCTCCTTACGaCaaGTgCcCAaCgTgTGcAAGATACCGTGGGCACGGGAAAAACTGTATTATAAGTAAATGCATGTATACTAAACTCACAAATTAGAGC
KIZ-R76W	TCTTAACCCAACTGCACAGAACAAAAACCTGCAGGAAACGAAGATAAATCatgAAGAATTATCTGAAGGAAATATGTGAATCTGAAAAGAAGGCTCATACTTGGAACCAAGAATATTTAAAGCGATTTGAGCGTGTCCAAGCTCATGTTGTACACtcgaaagctacatataaggaacgtgctgctactcatcctagtcctgttgc
KIZ-p.R76*	TCTTAACCCAACTGCACAGAACAAAAACCTGCAGGAAACGAAGATAAATCatgAAGAATTATCTGAAGGAAATATGTGAATCTGAAAAGAAGGCTCATACTTGAAACCAAGAATATTTAAAGCGATTTGAGCGTGTCCAAGCTCATGTTGTACACtcgaaagctacatataaggaacgtgctgctactcatcctagtcctgttgc
The 30nt+GR gRNA to the target KIZ-p.R76*	ttacagaaaagcaggctgggaagcatatttgagaagatgcggccagcaaaactaaAAATATTCTTGGTTcCAAGTATGAGCCTTCGGGTGGAATAGTATAACAATATGCTAAATGTTGTTATAGTATCCCACCTAAAACTGTATTATAAGTAAATGCATGTATACTAAACTCACAAA
The 60nt gRNA to the target KIZ-p.R76*	caaagggaagggatgctaaggtagagggtgaacgttacagaaaagcaggctgggaagcatatttgagaagatgcggccagcaaaactaaCGCTCAAATCGCTTTAAATATTCTTGGTTcCAAGTATGAGCCTTCTTTTCAGATTCACATAAAACTGTATTATAAGTAAATGCATGTATACTAAACTCACAAATTAGAGCTTCAATTTAATTATATCAGTTATTACCCGGGAATCTCGGTCGTAATGATT
The 60nt gRNA with mismatches to the target KIZ-p.R76*	gagggtgaacgttacagaaaagcaggctgggaagcatatttgagaagatgcggccagcaaaactaaCGCTCAAATCGCTTTAAATATgCacGccacCAtaccTcAgCCTTCTTTTCAGATTCACATAAAACTGTATTATAAGTAAATGCATGTATACTAAACTCACAAATTAG
TRPM1-K294W	ATGAAATTGCCCAGTATTCTTAACCCAACTGCACAGAACAAAAACCTGCAGGAAACGAAGATAAATCatgGTGATTTGTGATGGCAGCGGACGTGCCTCGGACATCCTGTCCTTTGCGCACTGGTACTGTGAAGAAGGCGGAATAATAAATGAGTCCCTCAGGGAGCAGCTTtcgaaagctacatataaggaacgtgctgctactcatcctagtcctgttgctgccaagctatttaata
TRPM1-p.K294*	ATGAAATTGCCCAGTATTCTTAACCCAACTGCACAGAACAAAAACCTGCAGGAAACGAAGATAAATCatgGTGATTTGTGATGGCAGCGGACGTGCCTCGGACATCCTGTCCTTTGCGCACTAGTACTGTGAAGAAGGCGGAATAATAAATGAGTCCCTCAGGGAGCAGCTTtcgaaagctacatataaggaacgtgctgctactcatcctagtcctgttgctgccaagctatttaata

The 30nt+GR gRNA to the target TRPM1-p.K294*	gaaaagcaggctgggaagcatatttgagaagatgcggccagcaaaactaaCTTCTTCACAGTACcAGTGCGCAAAGGACAGGGTGGAATAGTATAACAATATGCTAAATGTTGTTATAGTATCCCACCTAAAACTGTATTATAAGTAAATGCATGTATACTAAACTCACAAA
The 60nt gRNA to the target TRPM1-p.K294*	cgttacagaaaagcaggctgggaagcatatttgagaagatgcggccagcaaaactaaCATTTATTATTCCGCCTTCTTCACAGTACcAGTGCGCAAAGGACAGGATGTCCGAGGCACAAAACTGTATTATAAGTAAATGCATGTATACTAAACTCACAAATTAGAGC
The 60nt gRNA with mismatches to the target TRPM1-p.K294*	gaaaagcaggctgggaagcatatttgagaagatgcggccagcaaaactaaCATTTATTATTCCGCCTTCTTgAaAcTgCcAcTatGCgAAGGACAGGATGTCCGAGGCACAAAACTGTATTATAAGTAAATGCATGTATACTAAACTCACAAATTAGAGC
USH2A-W3955W	ATATATACGCATATGTGGTGTTGAAGAAACATGAAATTGCCCAGTATTCTTAACCCAACTGCACAGAACAAAAACCTGCAGGAAACGAAGATAAATCatgGACGAATATCGGGTCAGAGCCTGTAACTCCAAGGGTTCAGTGGAGAGTCTGTGGTCATTAACACAAACTCTGGAAGCTCCACCTCAAGATTTTCCAGCTCCTtcgaaagctacataaggaacgtgctgctactcatcctagtcctgttgctgccaagctatttaatatcatgcacgaaaagcaaacaaacttgtgtgctt
USH2A-p.W3955*	ATATATACGCATATGTGGTGTTGAAGAAACATGAAATTGCCCAGTATTCTTAACCCAACTGCACAGAACAAAAACCTGCAGGAAACGAAGATAAATCatgGACGAATATCGGGTCAGAGCCTGTAACTCCAAGGGTTCAGTGGAGAGTCTGTAGTCATTAACACAAACTCTGGAAGCTCCACCTCAAGATTTTCCAGCTCCTtcgaaagctacataaggaacgtgctgctactcatcctagtcctgttgctgccaagctatttaatatcatgcacgaaaagcaaacaaacttgtgtgctt
The 30nt+GR gRNA to the target USH2A-p.W3955*	aaagggaagggatgctaaggtagagggtgaacgttacagaaaagcaggctgggaagcatatttgagaagatgcggccagcaaaactaaGTTTGTGTTAATGACcACAGACTCTCCACTGGGTGGAATAGTATAACAATATGCTAAATGTTGTTATAGTATCCCACCTAAAACTGTATTATAAGTAAATGCATGTATACTAAACTCACAAATTAGAGCTTCAATTTAATTATATCAGTTATTACCCGGGAATCTCG
The 60nt gRNA to the target USH2A-p.W3955*	gaaaagcaggctgggaagcatatttgagaagatgcggccagcaaaactaaGTGGAGCTTCCAGAGTTTGTGTTAATGACcACAGACTCTCCACTGAACCCTTGGAGTTACAAAACTGTATTATAAGTAAATGCATGTATACTAAACTCACAAATTAGAGC
The 60nt gRNA with mismatches to the target USH2A-p.W3955*	gaaaagcaggctgggaagcatatttgagaagatgcggccagcaaaactaaGTGGAGCTTCCAGAGTTTGTGTAACGGCCcAGCGTCGCTCCACTGAACCCTTGGAGTTACAAAACTGTATTATAAGTAAATGCATGTATACTAAACTCACAAATTAGAGC

Target gene - blue
Reverse complement “tails” - yellow
Tail with “recruitment element” (GR) - green
The position of targeted A - red
Plasmid homology ends - purple

Table S3-NGS primers.

OSB ID	Name	Sequences
2795	Forward primer on the 60nt gRNA to the target FAM161A-p.R523* + sp p5 for deepseq	TCGTCGGCAGCGTCAGATGTGTATAAGAGACAG**atgCCTGTGCCTTGTAAC**
2796	Forward primer on the 60nt gRNA to the target TRPM1-p.K294* + sp p5 for deepseq	TCGTCGGCAGCGTCAGATGTGTATAAGAGACAG**atgGTGATTTGTGATGGCA**
2797	Forward primer on the 60nt gRNA to the target KIZ-p.R76* + sp p5 for deepseq	TCGTCGGCAGCGTCAGATGTGTATAAGAGACAG**atgAAGAATTATCTGAAGGAAATATGT**
2798	Reverse primer (for all the target) on URA3 39bp downstream to start codon + sp p7 for deepseq	GTCTCGTGGGCTCGGAGATGTGTATAAGAGACAG**atgagtagcagcacgttc**
2840	Forward primer on the 60nt gRNA to the target USH2A-p.W3955* + sp p5 for deepseq	TCGTCGGCAGCGTCAGATGTGTATAAGAGACAG**atgGACGAATATCGGGTCAGAG**
1202	Forward primer on URA3 173bp upstream to the A gRNA	GAGACGCATTGGGTCAACAG
502	Reverse primer on URA3 195bp downstream to the gRNA	CGACGGCCAGTGAATTGTAA
2366	Forward primer on URA3 300bp upstream to the target	aatttcacacaggaaacagctatg
207	Reverse primer on URA3 263bp downstream to the target	GTCAGCAAATTTTCTGTCTTCG
2874	Reverse primer for addition tail to the kiz's library with homologous to the 3' of URA3 in the BSB 704 plasmid.	GCTCTAATTTGTGAGTTTAGTATACATGCATTTACTTATAATACAGTTTT
2875	Forward primer for addition tail to the kiz's library with homologous to the 3' of URA3 in the BSB 704 plasmid.	gaaaagcaggctgggaagcatatttgagaagatgcggccagcaaaactaa

Table S4: Sequences of chemically modified gRNA

Key: (N)=RNA base, [N]=2'-OMe RNA base, *=Phosphorothioate linkage		
gRNA target	**Type**	**gRNA Sequence 5'-3'**
TRPM1 p.K294*	**60 bases**	[C*][A*][U*](UUAUUAUUCCGCCUUCUUCACAGUACCAGUGCGCAAAGGACAGGAUGUCCGAG)(G*)[C*][A*][C]
FAM161A p.R523*	**60 bases**	[T*][C*][C*](TCAAGTGATCTCCTTACGGCTTGTTCCCATCCTCTGGAAGATACCGTGGGCAC)(G*)[G*][G*][A]
KIZ p.R76*	**60 bases**	[C*][G*][C*](UCAAAUCGCUUUAAAUAUUCUUGGUUCCAAGUAUGAGCCUUCUUUUCAGAUUC)(A*)[C*][A*][U]
KIZ p.R76*	**"B4" 60 bases**	[C*][G*][C*](UGAAAUCGCUUUAAAUAUUCUUGGUUCCAAGUAUGUUCCUUCUUUUCAGAUUC)(A*)[C*][A*][U]
KIZ p.R76*	**"B12" 60 bases**	[C*][G*][C*](UCAAAUCGGUUCAAAUAUUCUUGGUUCCAAGUAUGUUCAUUCUUUUCAGAUUC)(A*)[C*][A*][U]
KIZ p.R76*	**"TT" 60 bases**	[C*][G*][C*](UCAAAUCGCUUUAAAUAUUCUUGGUUCCAAGUAUGUUCCUUCUUUUCAGAUUC)(A*)[C*][A*][U]
USH2A p.W3955*	**60 bases**	[G*][U*][G*](GAGCUUCCAGAGUUUGUGUUAAUGACcACAGACUCUCCACUGAACCCUUGGAG)(U*)[U*][A*][C]
USH2A p.W3955*	**30 bases + GR motif**	[G*][U*][U*][U*][GUGUUAAUGA](CCA)[CAGACUCUCCACU](GGG)[U](GGAA)[U](AG)[U](A)[U](AA)[C](AA)[U](A)[U](G)[CU](AAA)[U](G)[UU](G)[UU](A)[U](AG)[U](A)[UCCC](A)[C*][C*][U]

SUPPLEMENTAL FIGURES:

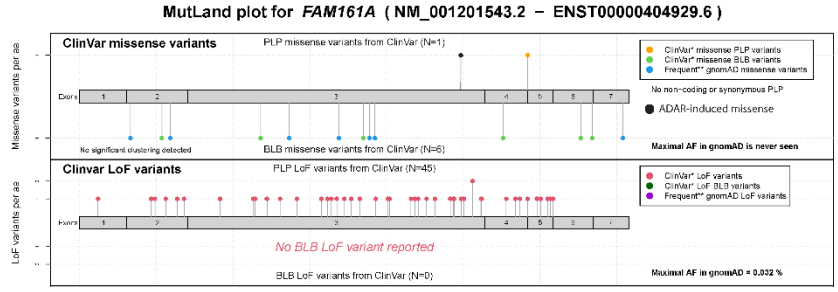

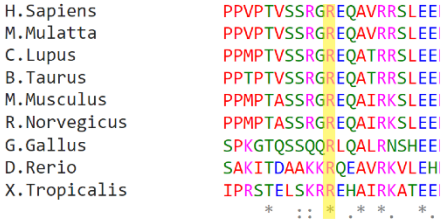

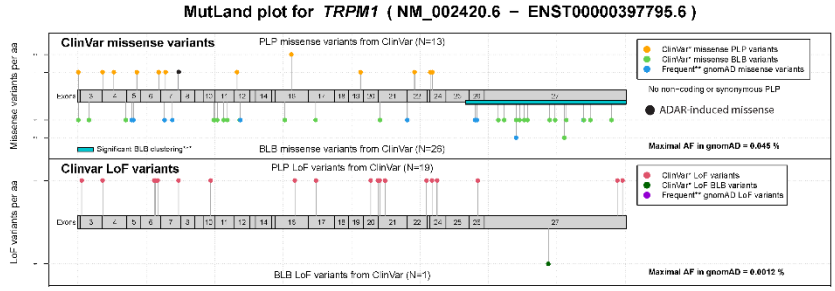

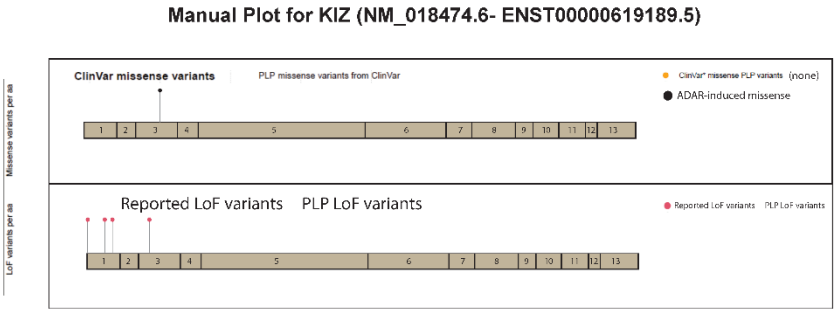

Figure S1. MutLand analysis and conservation of mutations in three genes. Left pane: MutLand plots for *FAM161A*, *TRPM1*, and *KIZ* (created manually due to lack of proper Annovar annotation for the *KIZ* gene) showing exonic location of pathogenic or likely pathogenic missense variants in these genes, as well as Clinvar LoF variants. The black circle was manually added to each plot to show where the ADAR-induced missense mutation would be found in each gene. Right pane: Conservation of amino acids in the regions flanking the ADAR targeted codon for each gene with the ADAR-edited amino acid highlighted in yellow

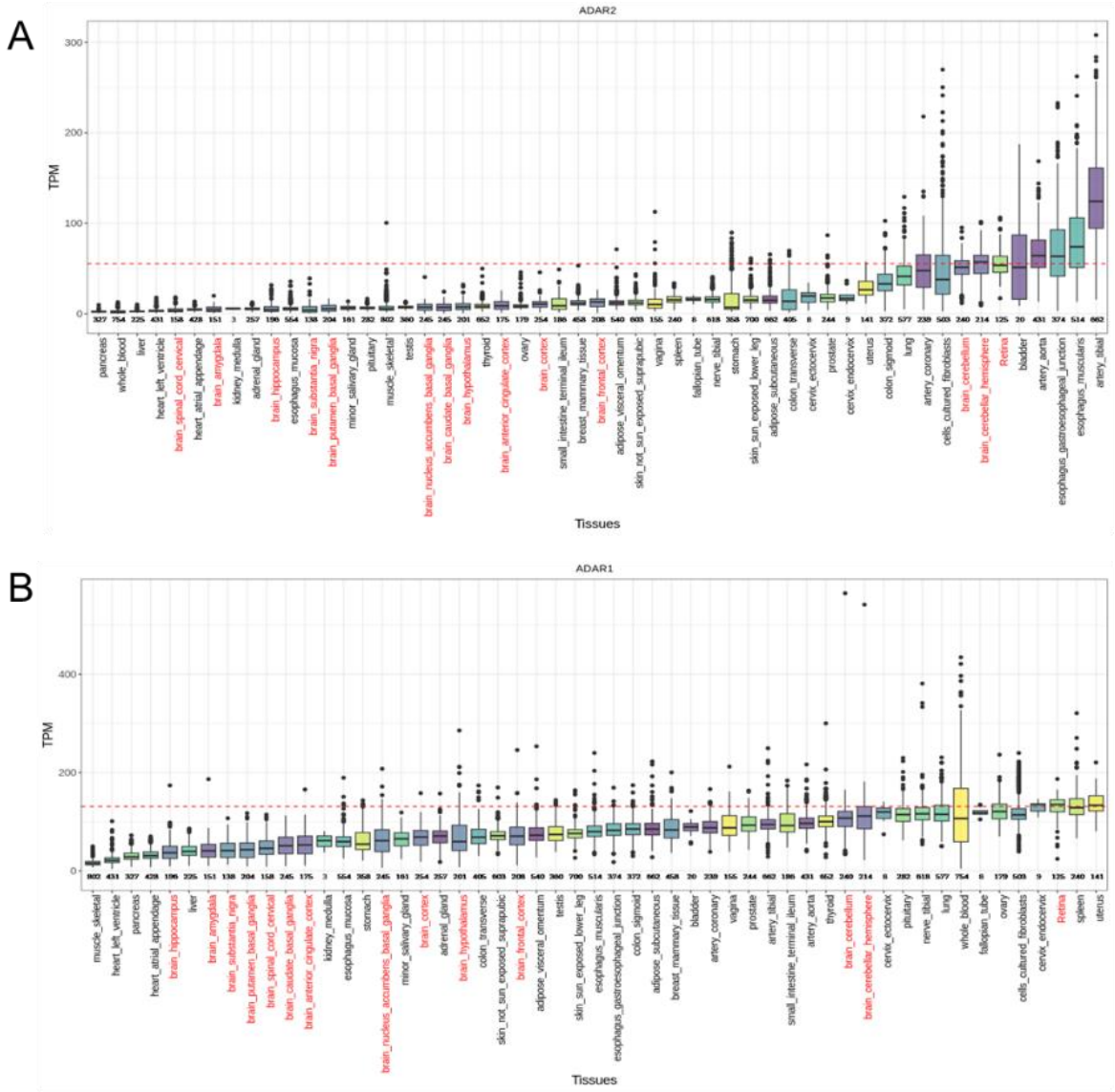
A
ADAR2
TPM
Tissues
B
ADAR1
TPM
Tissues
C
Editing Level
Neuronal tissues
Other tissues
Retina
AZIN1 chr6:102829408
AZIN1 chr8:102829409
BLCAP chr20:37519131
BLCAP chr20:37519161
BLCAP chr20:37519170
CACNA1D chr3:53786865
CADPS chr3:62438132
COG3 chr13:45516236
COPA chr1:160332454
CYFIP2 chr5:157309800
FLNA chrX:154351582
FLNB chr3:58156074
GABRA3 chrX:152189847
GRIA2 chr4:157336723
GRIA2 chr4:157336727
GRIA2 chr4:157360142
GRIA3 chrX:123465111
GRIA4 chr11:105933968
GRIK1 chr21:29581430
GRIK2 chr6:101889814
GRIK2 chr6:101889827
GRIK2 chr6:101924714
NOVA1 chr14:26448324
SON chr21:33550495
SON chr21:33551013
TMEM63B chr6:44152612
UNC80 chr2:209970889

Figure S2. Expression and editing levels of ADAR in the retina compared to various tissues. The presented analysis is based on data retrieved from the GTEx project [1] and a downloaded dataset (Bio Project: PRJNA476171, only samples exhibiting MGS level of zero or one were included) used for the retinal-related data. A&B). Expression levels of hADAR2 **(A)** and hADAR1 **(B)** across different tissues. Expression levels are depicted as transcript per million (TPM). The number of samples included for each tissue is indicated at the bottom of each graph. The dashed red line represents the mean expression levels in the retina. Neuronal tissues are highlighted in red. **(C)** Editing levels of conserved editing sites across 48 tissues. Editing levels for the retina were calculated based on the above-mentioned dataset, and editing levels for the other tissues were retrieved from [2]. Retinal and neuronal tissue-related data are marked in red and yellow, respectively. Each dot represents the combined data from all samples derived from a given tissue.

1. GTEx Consortium (2013). The Genotype-Tissue Expression (GTEx) project. Nat. Genet. *45*, 580–585. 10.1038/ng.2653.

2. Gabay, O., Shoshan, Y., Kopel, E., Ben-Zvi, U., Mann, T.D., Bressler, N., Cohen-Fultheim, R., Schaffer, A.A., Roth, S.H., Tzur, Z., et al. (2022). Landscape of adenosine-to-inosine RNA recoding across human tissues. Nat. Commun. *13*, 1184. 10.1038/s41467-022-28841-4.

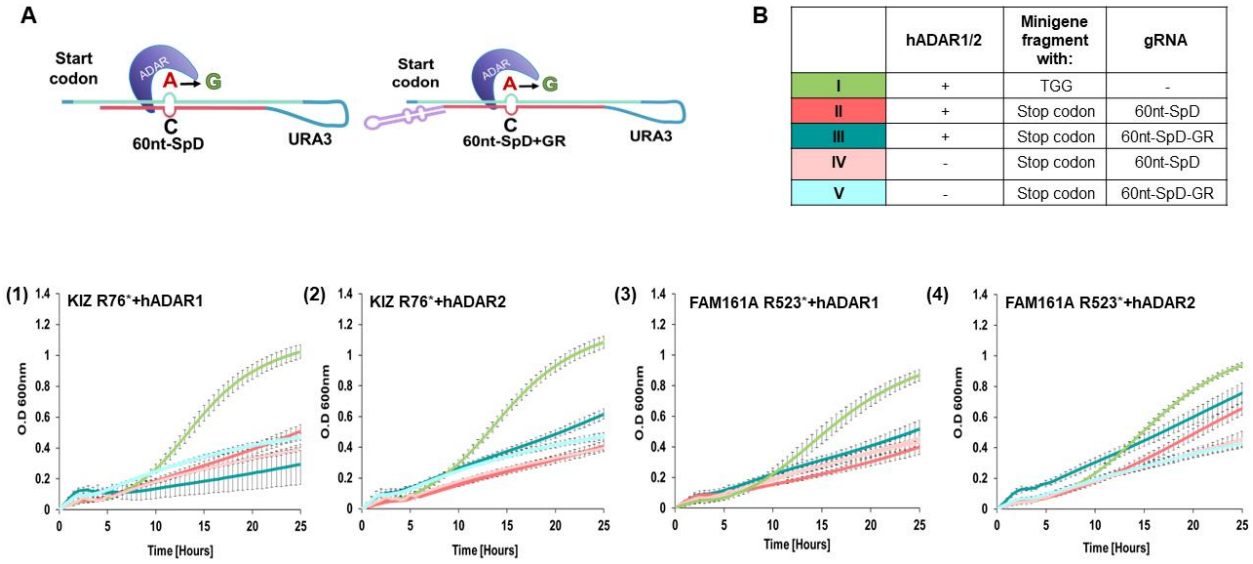

	hADAR1/2	Minigene fragment with:	gRNA
I	+	TGG	-
II	+	Stop codon	60nt-SpD
III	+	Stop codon	60nt-SpD-GR
IV	-	Stop codon	60nt-SpD
V	-	Stop codon	60nt-SpD-GR

Figure S3. No improvement in the growth of *KIZ*-p.R76* and *FAM161A* p.R523* mutants upon elongation of the 30nt specificity domain to 60nt. The experiments presented here are similar to those presented in Figure 3, however in the current experiments a longer specificity domain of 60nt (60nt-SpD-GR) was used instead of 30nt-SpD-GR gRNA .

A

B

	hADAR1/2	Minigene fragment with:	gRNA	Mismatches
I	+	Stop codon	60nt-SpD	-
II	+	Stop codon	60nt-SpD	+

C

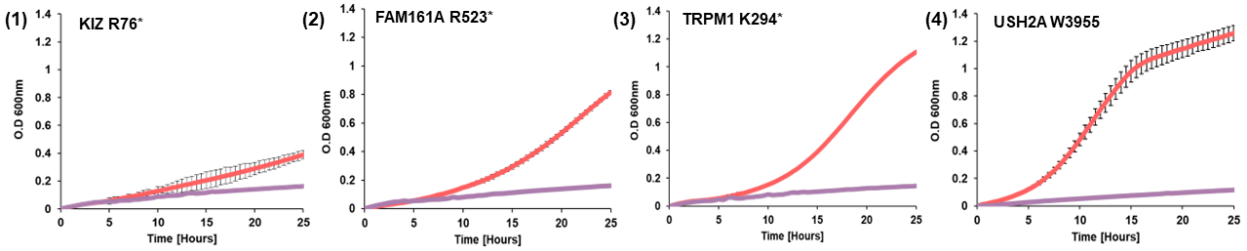

Figure S4. hADAR2-mediated editing of selected IRD mutations depends on the dsRNA **structure formed by the gRNA. (A)** Schematic representation of the dsRNA structure formed when the "tail" containing the selected gRNA sequences folds back at the RNA level on the target to form the dsRNA structure for ADAR recruitment, and of the control experiment that in addition to the A-C mismatch, carried additional mismatches around the target A. (B) A table describing the contents of the strains (denoted as I-II) tested in panels C-F. **(C)** Growth curves of the indicated strains were produced as described in Figure 2D.

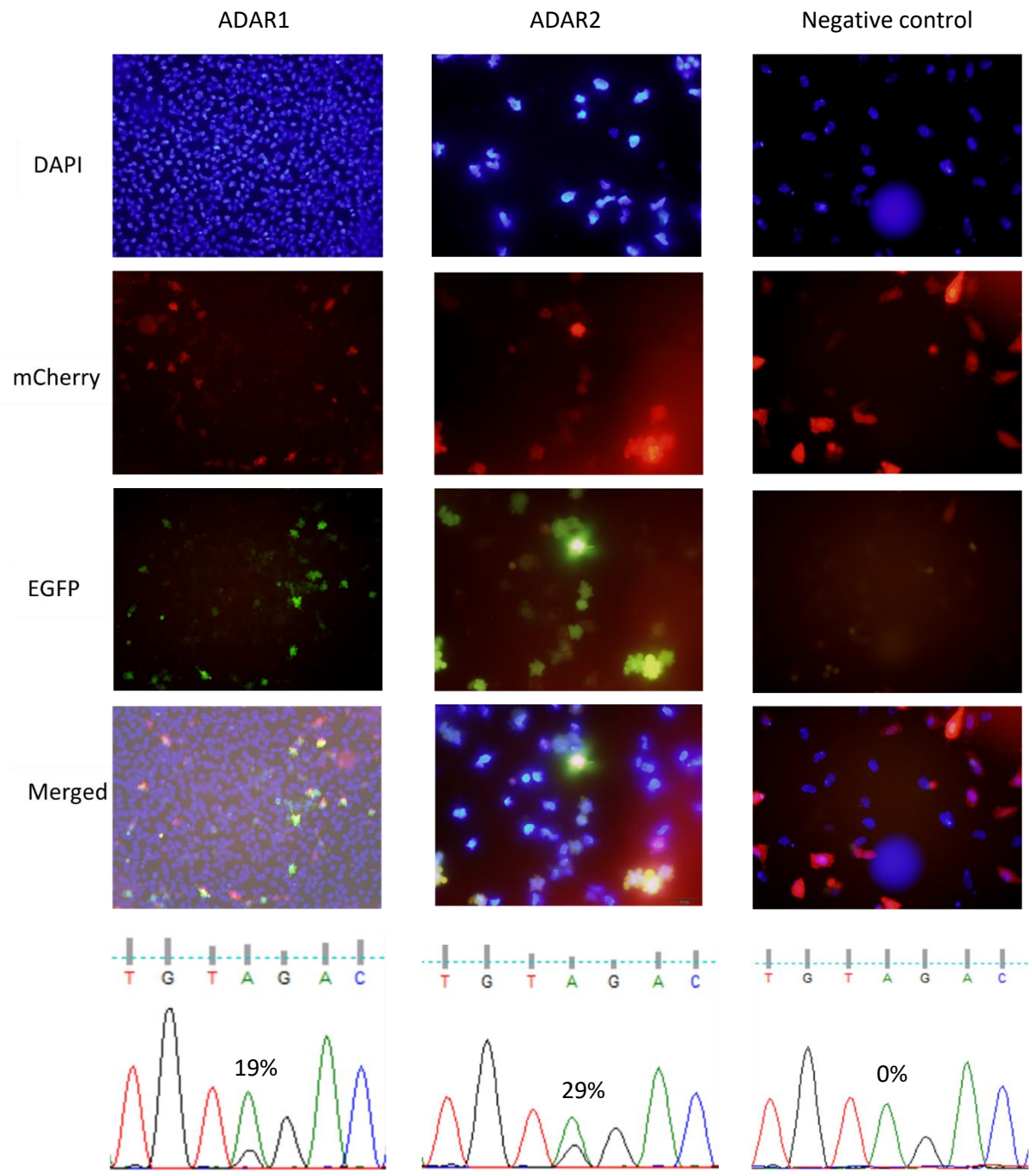

Figure S5: Confirmation of the reporter system. Representative images from samples of ADAR1 p.110 (ADAR1) and ADAR2 overexpressing HeLa cells transfected with both the 3'-UTR *GAPDH* nonsense mutation reporter plasmid and chemically modified gRNA (18 bp long complementarity region and a 55 bp GR motif tail) or no gRNA (negative control) at 96 hours post-seeding using fluorescent microscopy as well as representative Sanger sequences.

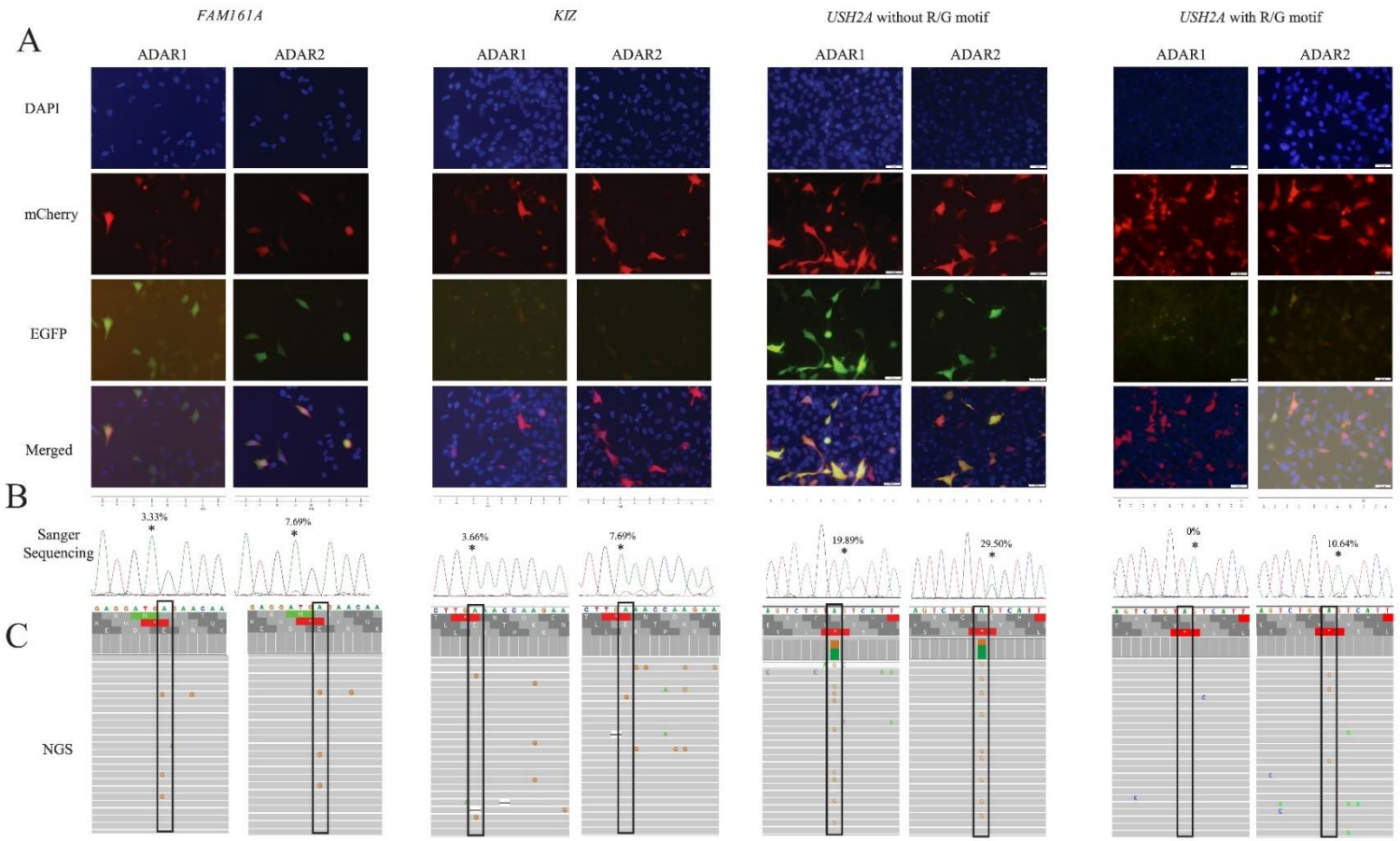

Figure S6: RNA editing of three IRD-causing mutations. Representative images from samples of ADAR1 p.110 (ADAR1) and ADAR2 overexpressing HeLa cells transfected with either the *FAM161A*, *KIZ*, or *USH2A* (with and without GR motif) nonsense mutation reporter plasmid and 60-mer chemically modified gRNA at 96 hours post-seeding. **(A)** Fluorescent microscopy **(B)** Sanger sequence **(C)** Next generation sequencing reads in IGV viewer

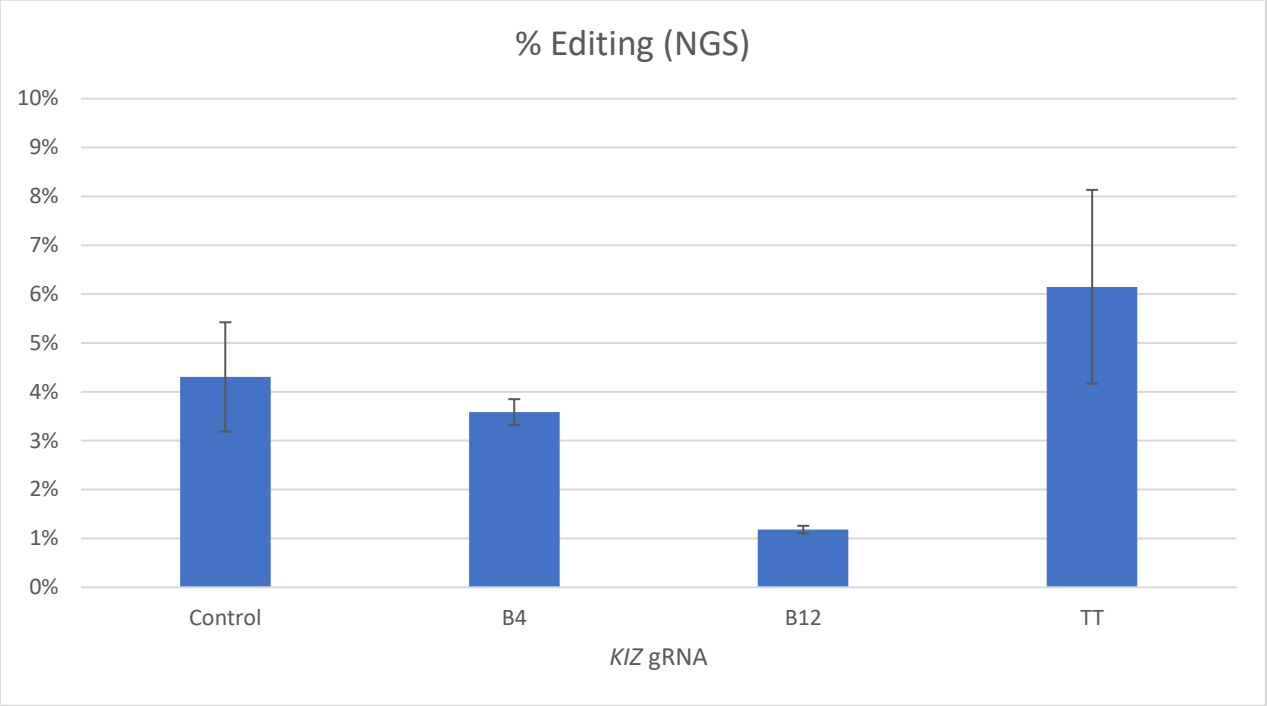

Figure S7: Editing levels of selected gRNAs. Editing levels of adenosine target in the *KIZ* minigene in ADAR2-expressing HeLa cells after introduction of B4, B12, or TT gRNA with multiple mismatches, corrected for background. Results are mean ± standard error of the mean (SEM n = 3).

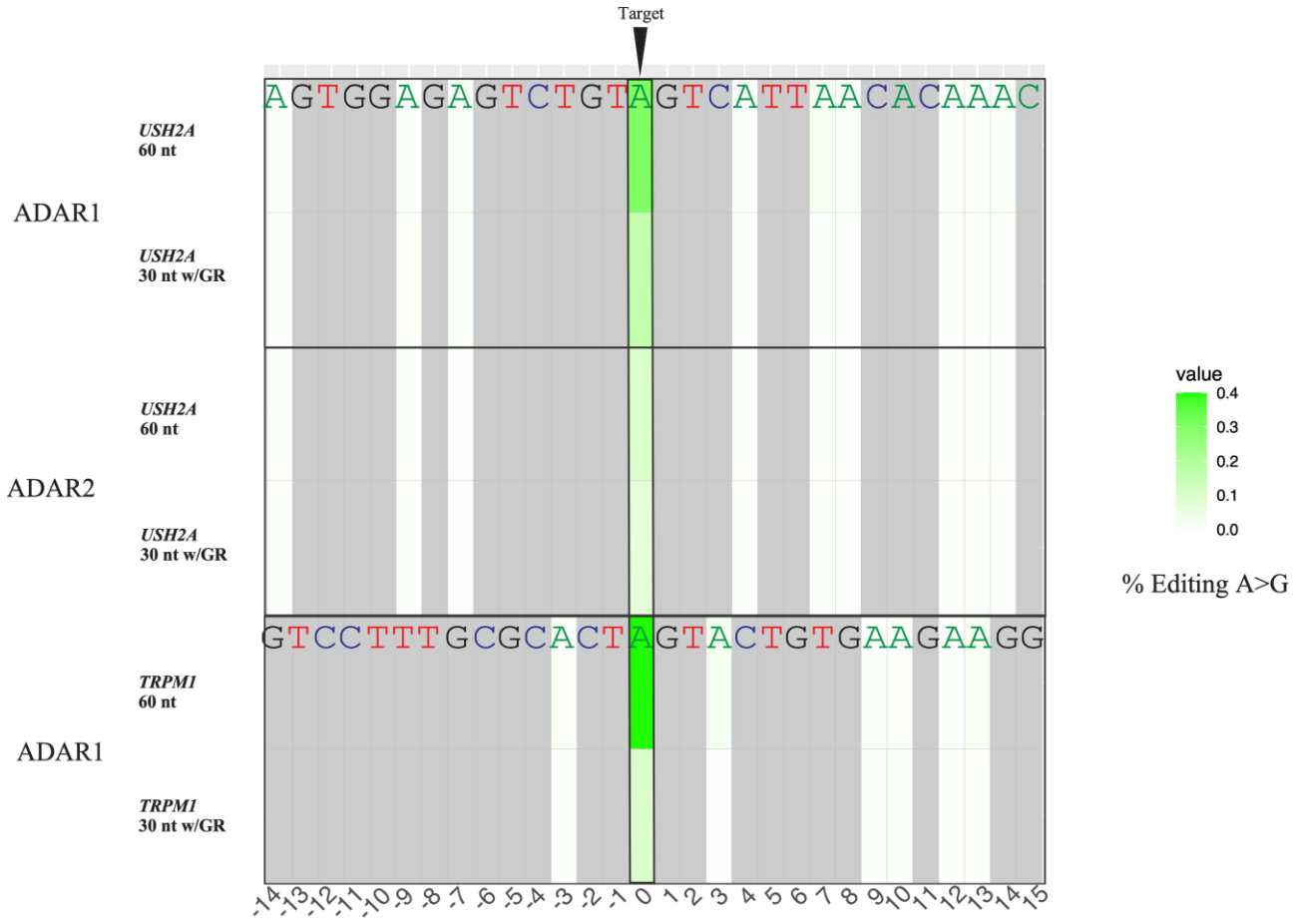

Figure S8: Heatmap off-target analysis of three IRD-causing mutations. Using shorter gRNAs can reduce bystander editing, but at the cost of potentially negatively impacting the target adenosine. Heatmap of average off-target and on-target editing rate for adenosines in the indicated strains. Average editing levels are shown are the result of NGS analysis (n=3). Positions below the heatmap are relative to the target adenosine (0), bases in grey are non-adenosine bases while adenosines with 0% editing are white gradually increasing to deep green in correlation with increasing editing levels.